QUARTERLY REPORT

April 1, 2021 – June 30, 2021

Kentucky Tobacco
Research & Development Center

College of Agriculture,
Food and Environment

UNIVERSITY OF KENTUCKY
College of Agriculture, Food and Environment

MEMORANDUM

DATE: July 27, 2021

TO: Kentucky Tobacco Research Board Members
Legislative Research Commission

FROM: Dr. Ling Yuan
Managing Director, KTRDC

SUBJECT: Kentucky Tobacco Research & Development Center
Quarterly Report for April 1, 2021 – June 30, 2021

Enclosed is a copy of the Kentucky Tobacco Research & Development Center's Quarterly Report for April 1, 2021 – June 30, 2021.

If you have any questions, please feel welcome to contact me at (859) 257-5798 or email lyuan3@uky.edu.

Enc.

TABLE OF CONTENTS

EXECUTIVE SUMMARY

Introduction

The legislation (KRS 248.510 - 248.580) which provides funds in support of the research programs at the Kentucky Tobacco Research and Development Center (KTRDC) requires that a quarterly research report be submitted to the Kentucky Tobacco Research Board (KTRB) and the Legislative Research Commission.

The overall reporting plan is:

January 1	-	March 31:	Selected topics
April 1	-	June 30:	Selected topics
July 1	-	September 30:	Selected topics
October 1	-	December 31:	Annual comprehensive report

As required by KRS 248.570, a financial report covering expenditures for the relevant proportion of the April 1, 2021 – June 30, 2021 fiscal year is included in this report.

The news and research publications provided in this quarterly report are a representative selection of the Center's output. For a full description of all KTRDC research and activities please refer to the KTRDC Annual Report.

Quarterly News

- Abstracts for both the CORESTA and TSRC conferences were submitted in May. A number of papers from KTRDC have been accepted. The University of Kentucky has the third highest number of papers submitted for the CORESTA conference in October.
- Normal operations at UK stopped in mid-March 2020, due to the pandemic. KTRDC staff continued to work through the pandemic, with strict precautions in place, as there were ongoing grants and many experiments which could not be halted. Those who could work from home did so, so that the number of people in the building was greatly reduced. Social distancing was observed, face masks were mandatory and lab staff were carefully spread out, rotating their hours and locations. In mid-June 2021, KTRDC staff members who were working remotely returned to the office, and normal operations resumed. Almost all KTRDC staff are now fully vaccinated against COVID-19.

- This quarter has been a busy time at the farm.
  - Activity in April was limited to the care of seedlings in the greenhouse.
  - May's activities mainly involved transferring seedlings into float trays in a predetermined sequence corresponding to the randomized order of treatments in the field, and transplanting. The first transplanting was done in the third week of May, and transplanting continued into June. Transplanting was considerably hampered by rain, and several experiments were set out later than planned as a result.
  - The *Artemisia annua* trials were transplanted in the second week in May.
  - Early sampling for burley, dark and cigar LC Foundation seed screening was done in June.
  - Efforts to regenerate the KTRDC *Nicotiana* species collection in the greenhouse began in June.
- The June board meeting was held via Zoom, because of the pandemic. The KTRDC Director, Ling Yuan, gave an update on the KTRDC activities and budget.
  - The total budget for 2021-2022 was in line with the fiscal year 2020-2021 budget. Actual income for 2021 was lower than projected.
  - Industry funding for research has been decreasing for several years and is not expected to be a significant source of revenue in coming years.
  - Dr. Yuan requested $110,000 in new funding for Summit grants for the coming fiscal year.
- The proficiency testing (PT) program continues to be well patronized.
  - The CIG-2021A round opened in January 2021 and closed in May. The interim report was issued in May and three labs requested the ability to submit revised data. The revised data was analyzed, and the final report was ready for review in June.
  - The CIG-2021B round opened in March 2021 and closed in July. The interim report is anticipated to be ready for review in early August and the final report will be ready for review in late August.
  - The CIG-2021C round opened in June 2021 and is scheduled to close in September 2021.
- Several new items have been added to the CTRP reference product collection.
  - CTRP introduced four reference cigars for research purposes in October 2019 to facilitate research and method development for cigars. These products

were used in the CORESTA Cigar Smoke Analysis 14th Collaborative Study, which was published in April 2021.

  - CTRP introduced a new ultra-low deliverable cigarette, the 2R5F, in November 2020. 2R5F filler was processed and ground for production of a new reference ground tobacco, RT 11, which was made available for sale in June 2021.

- Preparation and planning are underway for the workshop hosted by CTRP on August 29th, prior to the start of the 74th Tobacco Science Research Conference. At this workshop, we will discuss our proficiency testing program, certified reference products and the production of new reference materials to meet the needs of the tobacco research community.

- To date, the University of Kentucky, Center for Tobacco Reference Products (CTRP) has been awarded three FDA (Food & Drug Administration) grants to produce and distribute reference products, the first of which is now complete.
  - The second grant, to produce four smokeless reference products, should be completed by the end of 2021. The four products have been produced and certified, are being sold to research institutions around the world and are included in the proficiency testing program at CTRP. Our scientists are working to finalize several research projects on these products and presentations and publications are being produced. The CTRP is currently drafting the mid-year report for submission to the FDA in August.
  - The third grant for production of reference cigars has focused on the analysis of commercially available products in three categories: (1) filtered little cigars, (2) cigarillos, and (3) large, non-premium cigars. All of these products will be machine-made with an HTL (homogenized tobacco leaf) wrapper. The main achievements for this reporting period focus on the analysis of commercial cigar products, preparation of preliminary design specifications for these reference products, and discussions with four cigar manufacturers for the production of the three reference cigar products. We continue to work with the FDA and cigar manufacturers to finalize the designs of the products and anticipate manufacturing to begin on one or more products in the quarter October-December 2021.

- The CTRP continues to look for new grant opportunities to expand our capabilities and meet the evolving needs of the tobacco research community. In May 2021, the CTRP submitted a proposal to RFA-FD-22-002 Data Standards

for Tobacco Research and Scientific Review. The first aim of the grant is to engage key stakeholders in the identification of significant issues impacting the standardization and accurate reporting of scientific data for cigar products. The second aim is to develop and promote data standards and consistent terminology for collecting and reporting scientific data for cigar products and to unify the currently available standards and the newly developed standards, and to make the standards for data, terminology, and analytical methods available to the public. The FDA plans to award this grant in November 2021.

The KTRDC Quarterly Reports include copies and brief summaries of research done by KTRDC scientists. I would like to thank Dr. Sanjay Singh, Dr. Sitakanta Pattanaik and Dr. Colin Fisher for their help with writing the summaries.

Summary of Selected Research Topics

Report #1 "*Maleic hydrazide elicits global transcriptomic changes in chemically topped tobacco to influence shoot bud development.*" **Sanjay Singh**, Mitchell Richmond, Bob Pearce, Andy Bailey, **Xin Hou**, **Sitakanta Pattanaik** and **Ling Yuan**

This paper describes the effects of a systemic suckercide, maleic hydrazide (MH), on tobacco gene expression. This research is important because although MH has been used as a systemic suckercide for more than 50 years, the effect of MH on tobacco gene expression has not been studied. The major finding was that MH affects a wide range of biological processes in tobacco to inhibit sucker development. This finding is of interest because we identified several MH-responsive genes that can potentially be used to develop a chemical-free sucker control system by altering the expression of these genes.

Topping (removal of apical buds) and control of suckers (axillary shoots) are common agronomic practices that significantly impact the yield and quality of tobacco. Application of suckercides to tobacco plants following topping is an effective way to control sucker growth. However, our current knowledge of the influence of suckercide applications on gene expression and the underlying molecular mechanism of sucker control is limited. Maleic hydrazide (MH) is a commonly used suckercide that is absorbed by the leaves and translocated to the leaf axils, where it inhibits sucker growth. In this study, we analyzed the differential gene expression in apical and axillary buds of tobacco treated with or without MH. Our results showed that MH treatment significantly influences the expression of

genes related to the vegetative-reproductive phase transition, meristem maintenance, DNA metabolism, and defense response. Our results provide insights into the global changes in plant gene expression in response to suckercide treatment. Suckercide application is expensive and potentially generates undesirable or harmful chemical residues and pollutes soil and water. We identified several MH-responsive genes that can potentially be used to develop a chemical-free sucker control system by altering the expression of these genes.

Report #2 *"Rumen and serum metabolomes in response to endophyte-infected tall fescue seed and isoflavone supplementation in beef steers."* Taylor Ault-Seay, Emily Melchior-Tiffany, Brooke Clemmons, Juan Cordero, Gary Bates, James Klotz, **Huihua Ji**, Jack Goodman, Kyle McLean and Phillip Myer

This research investigated why a mixture of tall fescue and clover reduced the effects of toxicosis in cattle. This is important because the ergot alkaloids present in fungal endophyte-infected fescue reduces the weight gain and productivity of cattle. The major finding was that isoflavone, a compound produced by clover, counteracts the toxic effects of the ergot alkaloids produced by the fescue fungal endophyte. It was shown that the isoflavone produced by clover reduces, or even eliminates, many of the detrimental effects on cattle caused by the ergot alkaloid produced by the fescue endophyte.

The growth and drought tolerance of tall fescue is improved when it is infected with a fungal endophyte that also unfortunately produces an ergot alkaloid, which affects cattle in several ways. It reduces the animal's muscle development and its ability to gain weight, and it causes the animal's blood vessels to constrict so that the body temperature increases and reduces the reproductive fertility. Research has shown that one way to reduce the effect of the ergot alkaloid causing this toxicosis is for cattle to graze in pastures with a mixture of tall fescue and clover. This reduction of the toxic effect of the ergot alkaloid is thought to be the result of isoflavone compounds that are produced by the clover. This paper describes how this theory was tested and investigates how isoflavone affects the animal's metabolism.

Four groups of steers were each fed a different combination of tall fescue, with or without the infection of the fungal endophyte, and each of these two diets was fed with or without a medicinal grade isoflavone for three weeks. The concentration of

a wide range of compounds required for normal development of the animals, which are normally found in the rumen and blood, were analyzed. The results showed a complex interaction between the two fescue and two isoflavone treatments on a diverse array of blood and rumen constituents that are required to build muscle protein and regulate some hormones. This in turn was probably caused by the effect of the ergot alkaloid on the number and variety of the bacteria that do the digesting in the animal's rumen, and by isoflavone reducing the blood vessel-constricting effect of the ergot, especially around the intestines. This would result in increased blood flow to absorb nutrients. This group of scientists is now planning experiments to find the optimum dose of isoflavone.

Planta (2020) 252:64
https://doi.org/10.1007/s00425-020-03460-9

ORIGINAL ARTICLE

Maleic hydrazide elicits global transcriptomic changes in chemically topped tobacco to influence shoot bud development

Sanjay K. Singh[2] · Mitchell D. Richmond[1,4] · Robert C. Pearce[1] · William A. Bailey[1] · Xin Hou[2,3] · Sitakanta Pattanaik[2] · Ling Yuan[1,2]

Received: 24 June 2020 / Accepted: 12 September 2020

Abstract

Main conclusion **Transcriptomic analysis revealed maleic hydrazide suppresses apical and axillary bud development by altering the expression of genes related to meristem development, cell division, DNA replication, DNA damage and recombination, and phytohormone signaling.**

Abstract Topping (removal of apical buds) is a common agricultural practice for some crop plants including cotton, cannabis, and tobacco. Maleic hydrazide (MH) is a systemic suckercide, a chemical that inhibits shoot bud growth, used to control the growth of apical (ApB) and axillary buds (AxB) following topping. However, the influence of MH on gene expression and the underlying molecular mechanism of controlling meristem development are not well studied. Our RNA sequencing analysis showed that MH significantly influences the transcriptomic landscape in ApB and AxB of chemically topped tobacco. Gene ontology (GO) enrichment analysis revealed that upregulated genes in ApB were enriched for phosphorelay signal transduction, and the regulation of transition timing from vegetative to reproductive phase, whereas downregulated genes were largely associated with meristem maintenance, cytokinin metabolism, cell wall synthesis, photosynthesis, and DNA metabolism. In MH-treated AxB, GO terms related to defense response and oxylipin metabolism were overrepresented in upregulated genes. GO terms associated with cell cycle, DNA metabolism, and cytokinin metabolism were enriched in downregulated genes. Expression of KNOX and MADS transcription factor (TF) family genes, known to be involved in meristem development, were affected in ApB and AxB by MH treatment. The promoters of MH-responsive genes are enriched for several known *cis*-acting elements, suggesting the involvement of a subset of TF families. Our findings suggest that MH affects shoot bud development in chemically topped tobacco by altering the expression of genes related to meristem development, DNA repair and recombination, cell division, and phytohormone signaling.

Keywords Maleic hydrazide · Systemic suckercide · Chemical topping · RNA sequencing · Apical and axillary bud development · Phytohormones

Abbreviations

ABA	Abscisic acid
ACO	1-Aminocyclopropane-1-carboxylate oxidase
ACS	1-Aminocyclopropane-1-carboxylate synthase
AGL	Agamous-like

Communicated by Anastasios Melis.

Electronic supplementary material The online version of this article (https://doi.org/10.1007/s00425-020-03460-9) contains supplementary material, which is available to authorized users.

✉ Sitakanta Pattanaik
spatt2@uky.edu

✉ Ling Yuan
lyuan3@uky.edu

[1] Department of Plant and Soil Sciences, University of Kentucky, Lexington, KY 40546, USA

[2] Kentucky Tobacco Research and Development Center, University of Kentucky, Lexington, KY 40546, USA

[3] Department of Tobacco, College of Plant Protection, Shandong Key Laboratory of Agricultural Microbiology, Shandong Agricultural University, Tai`an 271018, China

[4] Canadian Tobacco Research Foundation, Tillsonburg, ON N4G 4H5, Canada

Published online: 24 September 2020

AOS	Allene oxide synthase
ApB	Apical bud
AxB	Axillary bud
ARR	*Arabidopsis* Response regulators
APRR	*Arabidopsis* Pseudo-response regulators
BARD1	Breast cancer-associated ring domain 1
BTB/POZ	Bric-à-brac, tramtrack and broad complex/poxvirus and zinc finger
CDC	Cell division control
Cdt1	Chromatin licensing and DNA replication factor 1
CK	Cytokinin
CPS	*ent*-Copalyl diphosphate synthase
CRF	Cytokinin response factor
DEG	Differentially expressed genes
Cul4	Uniculme4
DHAR	Glutathione-dependent dehydroascorbate reductase
ERF	Ethylene response factor
ET	Ethylene
FDR	False discovery rate
FPKM	Fragments per kilobase of gene per million reads mapped
GA	Gibberellin
GGDP	Geranylgeranyl diphosphate
GAox	GA oxidases
GO	Gene ontology
GST	Glutathione *S*-transferases
HK	Histidine kinase
HP	His-containing phosphotransfer protein
JA	Jasmonic acid
KNATM	KNOX *Arabidopsis thaliana* MEINOX
KNOX	Knotted1-like homeobox
KO	Ent-kaurine oxidase
KS	Ent-kaurene synthase
LAS	Lateral suppressor
MCM	Minichromosome maintenance
MH	Maleic hydrazide
NTPase	Nucleotide triphosphatases
ORC	Origin recognition complex
PR genes	Pathogenesis-related genes
PWMs	Position-specific weight matrices
RAX	Regulator of axillary meristems
RIN	RNA integrity number
REV	Revolute
ROX	Regulator of axillary meristem formation
RPN12A	Regulatory particle non-atpase 12A
SA	Salicylic acid
SAM	Shoot apical meristem
SAMT	Salicylic acid carboxyl methyltransferase
TB1	Teosinte branched 1
TF	Transcription factor
TS	Terpene synthase
TSS	Translation start site
TSNA	Tobacco-specific nitrosamines

Introduction

Removal of the apical buds or inflorescence, an agricultural practice termed topping, influences the quality and yield of a number of crop species, including tomato (Gianfagna et al. 1997; Logendra et al. 2004; Venezian et al. 2017), cotton (Yang et al. 2012b; Renou et al. 2011), sunn hemp (*Crotolaria juncea*) (Tripathi et al. 2013), fenugreek (*Trigonella foenum-graecum*) (Vasudevan et al. 2008), mustard (*Brassica* spp.) (Singh et al. 2011), apple (Cline and Bakker 2016), and okra (*Abelmoschus esculentus*) (Marie et al. 2007). Topping of tobacco (*Nicotiana tabacum* L.) plants is usually accomplished by manually or mechanically removing the top of each plant in an entire field. Apical buds are removed at the button stage to prevent the development of inflorescence and to allow the allocation of nutrients to the leaves. Topping results in increased leaf size, weight, nicotine content, and other chemical constituents (Fisher and Priest 2004; Tso 1990; Rao et al. 2003). Topping, however, stimulates the proliferation of axillary buds (A×B; also known as suckers). A×B growth affects water and nutrient allocation to the primary leaves and, thus, negatively impacts crop yield (Collins and Hawks 1993). Additionally, A×B growth affects both quality and quantity of marketable leaves in tobacco. Manual topping is labor intensive and expensive. Therefore, a non-traditional method of topping, "chemical topping" (untopped plants treated with chemicals that inhibit apical and axillary bud growth), has been explored to eliminate the need for manual topping to reduce the labor cost (Peek 1995; Richmond 2018). In addition, Richmond (2018) found that yield and leaf quality of MH-treated chemically topped burley tobacco are comparable to manually topped plants. Moreover, significant reductions in total tobacco-specific nitrosamine (TSNA) content in chemically topped plants compared to manually topped plants has also been reported (Richmond 2018).

Tobacco sucker control is usually achieved by application of suckercides (chemicals that inhibit AxB growth). Three types of chemicals used to control sucker growth are known as contact, local systemic, and systemic suckercides. Contact suckercides are not absorbed or translocated in plants requiring direct placement on the leaf axils. Local systemic suckercides are absorbed in the leaf axil and translocated to inhibit bud growth. Systemic suckercides do not need to be in direct contact with the suckers as they are absorbed by the leaves and translocated to the leaf axils, where they inhibit bud growth. Maleic hydrazide (MH; 1,2-dihydro–3,6,-pyridazinedione) is a plant growth regulator that is used for lawns, amenity turf, and fruits/vegetables including citrus, potatoes,

carrots, onions, shallots and garlic. MH is widely used in tobacco production as a systemic suckercide. MH is readily translocated through the plant vasculature and inhibits cell division, thus preventing the growth of newly developing suckers without hindering the growth of more mature leaves. MH acts as an antimitotic agent in axillary bud tissue (Clapp and Seltmann 1983). The gene regulatory network involved in meristem maintenance and development in plants has been extensively studied. Accumulating evidence suggests that transcription factors (TFs) and phytohormones, such as cytokinin, gibberellic acid, and auxin, play major roles in the developmental process. TFs belonging to families of R2R3 MYBs, GRAS domain protein, bHLH, KNOX and HD-ZIP have been characterized for their roles in meristem development and maintenance (Müller et al. 2006; Yang et al. 2012a; Yang and Jiao 2016). However, the molecular mechanism by which MH affects bud growth is poorly understood even though the mode of action of MH has been studied for more than 70 years (Naylor 1950). There are a few reports on the influence of topping and suckercides on gene expression in tobacco (Qi et al. 2012; Guo et al. 2011; Tang et al. 2012; Singh et al. 2015). Previously, we reported the influence of two different suckercides, local (flumetralin, e.g. *Flupro*, UPL NA Inc., King of Prussia, PA, USA) and contact-localized–systemic (C_8–C_{10}–C_{12} fatty alcohol, e.g. *Off-shoot T*, UPL NA Inc., King of Prussia, PA, USA) on differential gene expression in tobacco (Singh et al. 2015). The differentially expressed genes (DEGs), largely related to wounding, phytohormone metabolism and specialized metabolite biosynthesis, exhibit significant upregulation following topping but downregulation after suckercide treatments (Singh et al. 2015).

The systemic nature of MH makes it an ideal compound for use in chemical topping. Our primary objectives are to study the impact of MH on gene expression in chemically topped tobacco plants and to investigate the molecular mechanism of action of MH on apical bud (ApB) and A×B growth. Here, we analyzed global changes in gene expression in MH-topped burley tobacco using transcriptomic analysis and propose a possible molecular mechanism of action of MH on ApB and A×B shoot growth in plants. The information generated is useful for the identification of potential candidate genes involved in sucker formation and for the development of chemical-free sucker control system for tobacco in the future.

Materials and methods

Plant material, MH treatment and RNA sequencing

Burley tobacco (*Nicotiana tabacum* variety 'KT210 LC') plants were grown at the Agricultural Experiment Station Spindletop Farm near Lexington, Kentucky, USA. MH (Royal MH-30, 180 g a.i. liter^{-1}, UPL NA Inc., King of Prussia, PA, USA) was applied with a CO_2-pressurized sprayer calibrated to 468 L ha-$^{-1}$ with a directed three-nozzle row^{-1} configuration (TG3–TG5–TG3 coarse solid cone nozzles, TeeJet Inc., USA) at the 10% button stage. Based on our previous study on the effects of suckercides on tobacco gene expression (Singh et al. 2015), we collected ApB and AxB samples 24 h after MH application from the MH-treated and control plants (untreated), froze them immediately in liquid nitrogen and stored at − 80 °C until RNA extraction (Fig. S1).

Total RNA was isolated from 100 mg of ApB and A×B tissues using the RNeasy Plant Mini Kit (Qiagen, USA) following the manufacturer's instructions. Quality of the RNA samples was determined using an Agilent 2100 Bioanalyzer (Agilent Technologies, USA) and RNA samples with RNA integrity number (RIN) 8 or above were used for library preparation. For each tissue (with or without MH treatment), three libraries were constructed using independent RNA samples. The TruSeq RNA Sample Prep Kit (Illumina, USA) was used for making libraries according to the manufacturer's protocol. Individually indexed libraries were combined at equal proportions and loaded onto a single lane of a flow cell. A 50-cycle single-end sequencing run was performed on the Illumina HiSeq2500 at the Duke Center for Genomic and Computational Biology.

Data processing and gene expression quantification

Raw Illumina sequence reads were processed as described previously (Singh et al. 2015). In summary, raw Illumina sequence reads were filtered for low-quality reads using the prinseq-lite-0.20.426 (Schmieder and Edwards 2011). Preprocessed reads were assessed for quality control with systemPipeR (Backman and Girke 2016). Read mapping was performed by Bowtie2 (Langmead and Salzberg 2012) using the tobacco reference sequence downloaded from Sol Genomics Network database (Galperin et al. 2015). Differential gene expression analysis was carried out using the DESeq2 Bioconductor package in R (Love et al. 2014). The differentially expressed genes (DEGs) were identified using the following two criteria: (i) fold change ≥ 2 and (ii) false discovery rate (FDR) p value correction of ≤ 0.05. Heatmap was constructed using the ComplexHeatmap (Gu et al. 2016) function in R through the Bioconductor package (R Core Team 2020).

Functional annotation and gene ontology (GO) analysis

Functional annotation of DEGs was performed with eggNOG 4.5 (Huerta-Cepas et al. 2016) and InterPro

(Mitchell et al. 2015) databases. GO analysis of enriched functional categories was performed using BiNGO (version 2.44) (Maere et al. 2005) and visualized in Cytoscape (Shannon et al. 2003). The hypergeometric test with Benjamini and Hochberg's FDR correction was used to calculate overrepresented GO categories among DEGs, using a p value ≤ 0.05. Results from the gene list analyzed using BiNGO were summarized with REViGO by removing redundant GO terms (Supek et al. 2011). The Mercator tool was used to bin all genes according to hierarchical ontologies and MapMan (v.3.5.1) was used to visualize DEGs on different pathways (Thimm et al. 2004).

Real-time quantitative PCR (RT-qPCR) analysis

We isolated RNA from control and MH-treated samples, and reverse-transcribed using Superscript III Reverse Transcriptase (Invitrogen, USA), following the manufacturer's instructions. Real-time quantitative PCR (RT-qPCR) was performed as previously described (Pattanaik et al. 2010). The comparative cycle threshold (Ct) method was used to measure transcript levels. Tobacco elongation factor-1α (GenBank accession number D63396) was used as a reference gene. Gene-specific primers used for RT-qPCR analysis are given in Table S1.

Motif enrichment analysis

The promoters (1 kb upstream of the translation start sites; TSS) of DEGs were scanned with PSCAN (Zambelli et al. 2009) to identify statistically overrepresented motifs. Motifs corresponding to known TF-binding sites and position-specific weight matrices (PWMs) were collected from the JASPAR database (Khan et al. 2018). Promoters were also scanned for the presence of TF binding motifs in the PLACE database (Higo et al. 1999) using the AME program (McLeay and Bailey 2010). Any PWM and motifs showing a P value equal or lower than 1E-5 were considered as significantly overrepresented.

Statistical analysis

For RNA sequencing, three independent biological replicates were used for control or MH-treated ApB or AxB (Table S2). The RT-qPCR experiments were performed using cDNA from three independent biological replicates and the error bars represent the means ± SD from three replicates. Statistical significance was calculated using the Student's t test: *, $P < 0.05$.

Results

RNA-seq analysis reveals differential gene expression between apical and axillary buds

RNA-seq analysis was performed to study the influence of MH on gene expression in ApB and AxB of chemically topped tobacco plants. A total of 12 samples comprised of control and MH-treated ApB and AxB were used for library preparation and sequencing using the Illumina HiSeq2500 system (Fig. S1). Sequencing of RNA libraries from ApB and A×B of tobacco generated a total of 450 million (M) clean reads (Table S2). Each biological replicate (control and MH-treated) was represented by an average of more than 100 M reads. On an average, more than 75% of the total reads from control and MH-treated libraries were successfully mapped to the reference tobacco genome sequence (Table S2). Transcripts with FPKM (Fragments Per Kilobase of gene per Million reads mapped) value ≥ 1 was included in our analysis. Total number of transcripts varied from approximately 44,000 to 47,000 in all analyzed samples which were further divided into three categories, low (1–5 FPKM), moderate (5–20 FPKM), or high (> 20 FPKM), based on their abundance. Both control and MH-treated samples had similar distribution of low, moderate, and highly expressed mRNAs (Fig. 1a) and about 10,000 mRNAs showed distinct accumulation patterns between MH-treated (chemically topped: CT) ApB and AxB with (CT-ApB and CT-AxB) and control (C-ApB and C-AxB) MH treatment (Fig. 1b).

MH treatment significantly alters gene expression in apical and axillary buds

Compared with the control, chemical topping significantly altered gene expression in ApB and AxB. A total of 573 (132 upregulated, 441 downregulated) and 2,632 (2,174 upregulated, 458 down-regulated) genes were found to be differentially expressed in chemically topped ApB and AxB, respectively (Fig. 2a; Table S3). A total of 87 genes common to both ApB and AxB were affected by MH treatment (Fig. 2b). Among the 87 genes, 8 were upregulated and 18 downregulated; the downregulated genes are enriched for meristem development and cytokinin (CK) metabolism. The downregulated genes in both MH-treated ApB and AxB included a number of the Knotted1-like homeobox (KNOX) family and BTB/POZ (bric-à-brac, tramtrack and broad complex/poxvirus and zinc finger) domain TFs. Members of both TF families are known to regulate the meristematic activities in plants (Gao et al. 2015; Tavakol et al. 2015). The other 61 genes showed

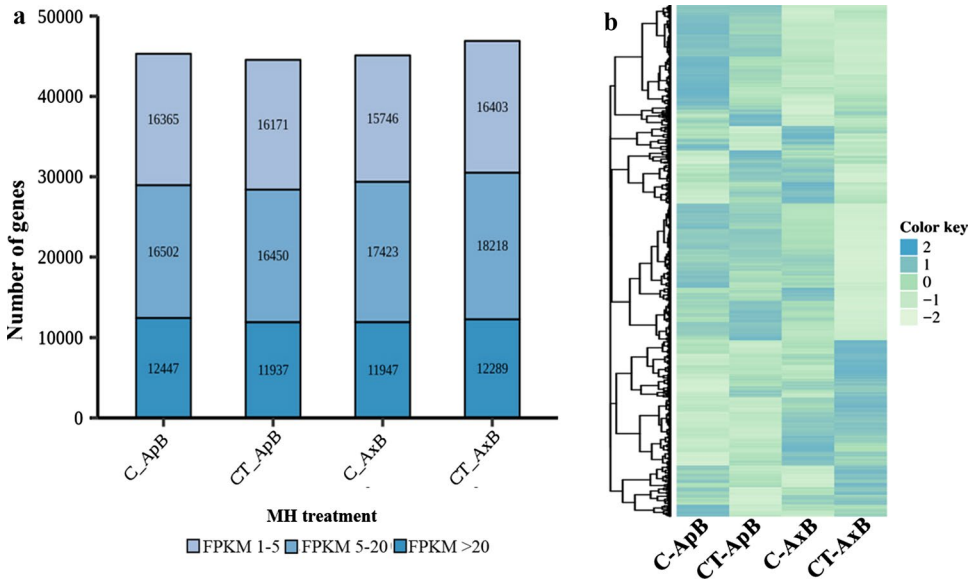

Fig. 1 Overview of RNA sequencing analysis. **a** Distribution of FPKM normalized transcripts across the axillary and apical bud tissue of MH-treated (chemically topped) and untreated (control) plants. **b** Clustered heat map of the top 10,000 highly abundant mRNAs. C-ApB, control apical bud; CT-ApB, chemically topped-apical bud; C-AxB, control axillary bud; CT-AxB, chemically topped-axillary bud

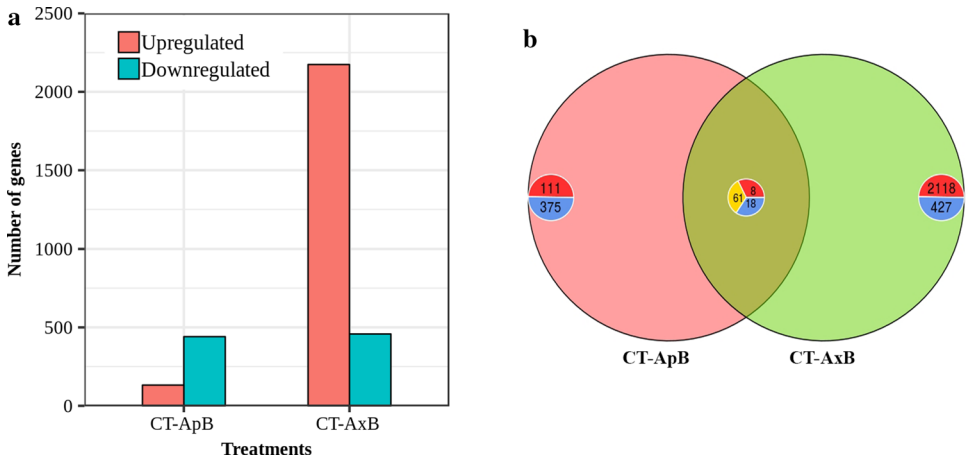

Fig. 2 Differentially expressed genes in **maleic hydrazide (MH)**-treated apical and axillary buds. **a** Number of upregulated and downregulated genes. **b** Venn diagram depicting the overlap of differentially expressed genes (DEGs) between MH-treated apical and axillary bud. CT-ApB, chemically topped-apical bud; CT-AxB, chemically topped-axillary bud

contra regulation (opposite regulation) in ApB and AxB. Genes related to secondary metabolism and defense, pathogenesis-related (PR) genes, chitinase and hormone biosynthesis (jasmonate and ethylene biosynthetic genes) were upregulated in MH-treated AxB but downregulated in ApB. Genes related to translation (e.g. ribosomal protein L22p/L17e family genes) were upregulated in MH-treated ApB. Differentially expressed genes are listed in Table S3.

Gene ontology enrichment analysis highlights the influence of MH on different developmental and metabolic pathways in ApB and AxB

To gain further insight into the effects of MH treatment, we performed gene ontology (GO) enrichment analysis to further examine the effect of MH treatment on genes that were differentially expressed in ApB and AxB (Fig. 3a, b). Genes upregulated in MH-treated ApB were enriched for the phosphorelay signal transduction system (GO:0,000,160) and regulation of gene expression (GO:0,010,468), while downregulated genes were enriched in GO terms related to meristem maintenance, cytokinin (CK) metabolism, cell wall synthesis, photosynthesis and DNA metabolism (Fig. 3a). The GO terms "phosphorelay signal transduction system" (GO:0,000,160) and "regulation of gene expression" (GO:0,010,468) include genes involved in CK signaling such Type-A Response Regulators (RR) and Cytokinin Response Factors (CRFs). Type-A RR and CRFs are negative regulators of CK signaling and were induced by MH application in ApB. The GO term meristem maintenance includes genes from the KNOX TF family, MADS gene family (Agamous-like; AGL), WUSCHEL-related homeobox 8, YABBY family (CRABS CLAW, CRC), and REPLUMLESS (RPL), which are well characterized for their roles in meristem, embryo and flower development (Khan et al. 2015;

Fig. 3 Gene ontology (GO) analyses of DEGs in **maleic hydrazide (MH)**-treated apical and axillary buds. GO analysis of DEGs in apical (**a**) and axillary bud (**b**). Upregulated GO terms are colored in 'red' while downregulated terms are in 'green'. Each circle represents one GO term. Circle size represents the number of genes in each GO category while color represents the significance level. Description of the GO terms in apical buds: GO:0,048,440 carpel development; GO:0,010,073 meristem maintenance; GO:0,042,219 cellular amino acid derivative catabolic process; GO:0,071,554 cell wall organization or biogenesis; GO:009,690 cytokinin metabolic process; GO:009,832 plant-type cell wall biogenesis; GO:0,010,468 regulation of gene expression; GO:006,355 regulation of transcription DNA-templated; GO:0,051,273 beta-glucan metabolic process; GO:0,009,808 lignin metabolic process; GO:0,080,027 response to herbivore; GO:0,015,979 photosynthesis; GO:0,000,160 two-component signal transduction (phosphorelay); GO:0,055,114 oxidation reduction process; GO:0,019,748 secondary metabolic process. Description of the GO terms in axillary buds: GO:0,019,321 pentose metabolic process; GO:0,007,049 cell cycle; GO:0,055,114 oxidation reduction process; GO:0,046,395 carboxylic acid catabolic process; GO:0,031,407 oxylipin metabolic process; GO:0,009,694 jasmonic acid metabolic process; GO:0,009,690 cytokinin metabolic process; GO:0,048,544 recognition of pollen; GO:006,259 DNA metabolic process; GO:0,006,260 DNA replication; GO:0,042,127 regulation of cell proliferation; GO:0,009,607 response to biotic stimulus; GO:0,006,952 defense response; GO:0,006,974 response to DNA damage stimulus; GO:0,034,421 post-translational protein acetylation; GO:0,009,744 response to sucrose; GO:0,006,468 protein phosphorylation; GO:0,006,807 nitrogen compound metabolic process; GO:0,000,003 reproduction; GO:0,035,428 hexose transmembrane transport

Gao et al. 2015; Borner et al. 2000; Goldshmidt et al. 2008; Leibfried et al. 2005). GO terms plant-type cell wall biogenesis (GO:0,009,832), lignin metabolism (GO:0,009,808) and oxidation–reduction (GO:0,055,114) include genes belonging to families of cellulose synthase, cytochrome P450, and laccase. These genes were mostly downregulated following MH treatment. MADS and KNOX family genes were also abundant in 'regulation of transcription DNA-templated' (GO:0,006,355) GO term and downregulated following MH treatment.

In MH-treated AxB, GO terms related to defense responses and oxylipin metabolism were enriched in upregulated genes, whereas cell cycle and DNA metabolism, and CK metabolism were enriched in downregulated genes (Fig. 3b). Cell division and cell elongation are two key aspects of plant growth. DNA replication is a complex and stringently regulated process that is limited to the S-phase of cell cycle. DNA replication consists of two key steps: formation of pre-replication complex (pre-RC) and the initiation of DNA replication. A number of proteins including Origin Recognition Complex (ORC), Cell Division Control (CDC) 6/CDC18, chromatin licensing and DNA replication factor 1 (Cdt1), and minichromosome maintenance (MCM) proteins are essential for the pre-RC formation (Gutierrez 2009). Expression of genes belonging to MCM (MCM2/3/5), ORC and CDC families, which are essential for initiation of DNA replication, was downregulated in MH-treated A×B. In addition to CDCs and MCMs, members of nucleotide triphosphatases (NTPases), such as replication factor C, were also suppressed by MH treatment. The Replication Protein A1B, RAD21.2, ARABIDOPSIS HOMOLOG OF YEAST CDT1 A, BREAST CANCER ASSOCIATED RING DOMAIN 1 (BARD1) and RECQ helicase l1 are known regulators of DNA repair and recombination in plants. Expression of these genes was suppressed in ApB and A×B by MH treatment. Several other genes

including *REGULATORY PARTICLE NON-ATPASE 12A* (RPN12A) (Smalle et al. 2002), Chromatin Assembly Factor-1 (CAF-1), FUSED (Oh et al. 2014) and ASF1-like histone chaperone (Lario et al. 2013), with known functions in CK signaling, cytokinesis and DNA replication and repair (Muñoz-Viana et al. 2017) were downregulated in MH-treated AxB. Collectively, these findings suggest that MH suppresses DNA replication, DNA repair, and recombination machinery, resulting in arrest of cell cycle and, ultimately, bud development. Moreover, MH inhibits apical and axillary shoot development possibly by affecting CK metabolic processes in tobacco. A complete list of GO terms is given in Supplementary Table S4.

MH-treatment alters the expression of TF genes involved in meristem development, defense responses and secondary metabolism

TFs belonging to R2R3MYBs, bHLH, GRAS, HD/ZIP, KNOX and BTB/POZ families play crucial roles in meristem maintenance and development in plants. The R2R3 MYB, Blind (BL)/Regulator of Axillary Meristems (RAX), bHLH TF Regulator of Axillary Meristem Formation (ROX) (Yang et al. 2012a), GRAS family TF Lateral suppressor (LAS) (Yang and Jiao 2016), and HD/ZIP TF Revoluta (REV), are positive regulators of axillary meristem development in *Arabidopsis*, tomato and pepper (Müller et al. 2006). Our transcriptome analysis revealed that the expression of the tobacco homologues of *BL*, *ROX*, and *LAS* was altered in the ApB and/or AxB after MH treatment (Table S5). In addition, expression of TFs belonging KNOX, MADS and BTB/POZ domain families was also affected by MH treatment both in ApB and AxB.

Notably in MH-treated ApB, expression of several MADS-box family TFs was downregulated (Fig. S2a). MADS-box family genes regulate both flowering time and vegetative to reproductive phase transition (Borner et al. 2000; Putterill et al. 2004). In *Arabidopsis,* flowering is proposed to be regulated by four genetic pathways, photoperiod, autonomous, vernalization, and gibberellin-induced pathways (Bäurle and Dean 2006; Boss et al. 2004). In the current ABCDE model for flower development, floral organ identity is specified by five classes of homeotic genes, A (APETALA1, AP1), B (PISTILATA, PI), C (AGAMOUS, AG), D (SEEDSTICK/AGAMOUS-LIKE11,STK/AGL11) and E (SEPALLATA, SEP) (Rijpkema et al. 2010). Different combinations of these homeotic genes determine the identities of the floral organs: sepals (A + E), petals (A + B + E), stamens (B + C + E), carpels (C + E), and ovules (D + E). In *Arabidopsis*, most members of class A, B, C, D, E belong to the MADS-box TF family. Since a large number of MADS-box genes were differentially expressed in MH-treated ApB, we analyzed the expression of homologs of well-characterized MADS-box family members in our transcriptome. SEPALLATA1 (SEP1), SEP2 and SEP3, and SEP4 are required to specify petals, stamens, and carpels (Ditta et al. 2004). Expression of several *SEP* homologs was repressed by MH application. In addition, expression of genes required for floral organ identity including *PISTILLATA*, *AGAMOUS, AP1,* and *AP3*, was also repressed by MH treatment. In *Arabidopsis*, AGAMOUS-like 22 (AGL22) regulates flowering time by negatively regulating the expression of the floral integrator, *FT*, via direct binding to the CArG motifs in the FT promoter region (Lee et al. 2007). AGL22 was induced in ApB by MH-treatment (Hartmann et al. 2000). Notably, a MADS-box TF, AGL6, which is reported to be a positive regulator of axillary meristem formation and flowering (Huang et al. 2012; Koo et al. 2010), is also repressed by MH application. In *Arabidopsis,* the BTB/POZ domain TFs, BLADE ON PETIOLE 1 (BOP1) and BOP2, act redundantly to control leaf and floral patterning by modulating the meristematic activity. BOP2 is highly expressed in the young floral meristem (Xu et al. 2010). Expression of BOP2 was repressed by MH treatment. The *Uniculme4* (*Cul4*) gene, a homolog of *Arabidopsis* BOP2, has also been shown to express in axil and leaf boundary regions to positively control AxB growth (Tavakol et al. 2015). Downregulation of multiple MADS-box and BTB/POZ family genes after MH application was consistent with previous findings that show MH treatment delays or inhibits flower initiation in several plants including tobacco (Klein and Leopold 1953; Naylor 1950).

In addition to meristem development, MH treatment also affected defense response and secondary metabolism. In MH-treated AxB, expression of TFs belonging to WRKY, AP2/ERF and NAC families were affected (Fig. S2b). WRKYs are well-studied plant-specific TFs involved in diverse biotic and abiotic stress responses as well as in developmental/physiological processes (Phukan et al. 2016). In addition, WRKY are key regulators of secondary metabolites in plants (Schluttenhofer and Yuan 2015). Expression of several WRKY TF genes, including *WRKY2, WRKY6, WRKY7, WRKY11, WRKY23, WRKY28, WRKY33, WRKY38, WRKY40, WRKY41, WRKY45, WRKY50, WRKY51, WRKY53, WRKY70*, was upregulated in MH-treated AxB. Previous studies in *Arabidopsis* suggest that WRKY50 and WRKY51 act as positive regulators of salicylic acid (SA)-mediated signaling and negative regulators of JA signaling (Gao et al. 2011). WRKY28 and WRKY70 are involved in both SA and JA signaling pathways in plants (Li et al. 2004; Chen et al. 2013). WRKY33 is a key regulator of camalexin biosynthesis and is required for resistance to necrotrophic fungal pathogens in *Arabidopsis* (Liu et al. 2016; Zheng et al. 2006). WRKY13, which is known to activate lignin biosynthesis (Li et al. 2015) and repress flowering (Li et al.

2016) in *Arabidopsis*, was upregulated by MH treatment in AxB.

MH perturbs the expression of KNOX family TFs involved in meristem maintenance and development

As expression of a number of KNOX family genes were altered by MH treatment, we analyzed in detail KNOX TF family in tobacco. The KNOX genes comprise a small family of TALE homeobox TFs that are found in all plant species and can be divided into two major sub-classes (Gao et al. 2015). Class I KNOX genes are most similar to maize *knotted1 (kn1)* gene and are predominantly expressed in the shoot apical meristem (SAM) (Gao et al. 2015; Hake et al. 2004). Class II KNOX genes exhibit diverse expression patterns (Gao et al. 2015). *KNOX ARABIDOPSIS THALIANA MEINOX (*KNATM*)* genes are relatively new members of the KNOX family which encodes a MEINOX domain but not a homeodomain. In *Arabidopsis*, KNATM is expressed in proximal-lateral domains of organ primordia and at the boundary of mature organs, and involved in leaf proximal–distal patterning (Magnani and Hake 2008). We identified 19 KNOX family members in tobacco and phylogenetic analysis revealed three major clades, class I KNOX, class II KNOX and KNATM (Fig. 4a), as described previously (Gao et al. 2015). The class I clade has eleven members and MH-treatment repressed the expression of most class I KNOX genes in ApB and AxB whereas expression of six class II KNOX genes were not significantly affected (Fig. 4b). Unlike typical KNOX family members, KNATM encodes a MEINOX domain without a homeodomain, and interacts with TALE-class homeodomain proteins to modulate their activities (Magnani and Hake 2008). We identified two KNATM family members in tobacco and both copies of KNATM were upregulated in ApB but not in AxB (Fig. 4b).

MH-treatment affects expression of other phytohormone biosynthetic and signaling genes in apical and axillary buds

We identified all phytohormone metabolism and signaling-related genes in tobacco as described previously (Table S6) (Prasad et al. 2016) and analyzed their expression in our transcriptome. In addition to CK, genes related to biosynthesis and signaling of a number of other phytohormones such as gibberellic acid (GA), JA, ethylene (ET), abscisic acid (ABA), and SA, were affected by MH-treatment in ApB and

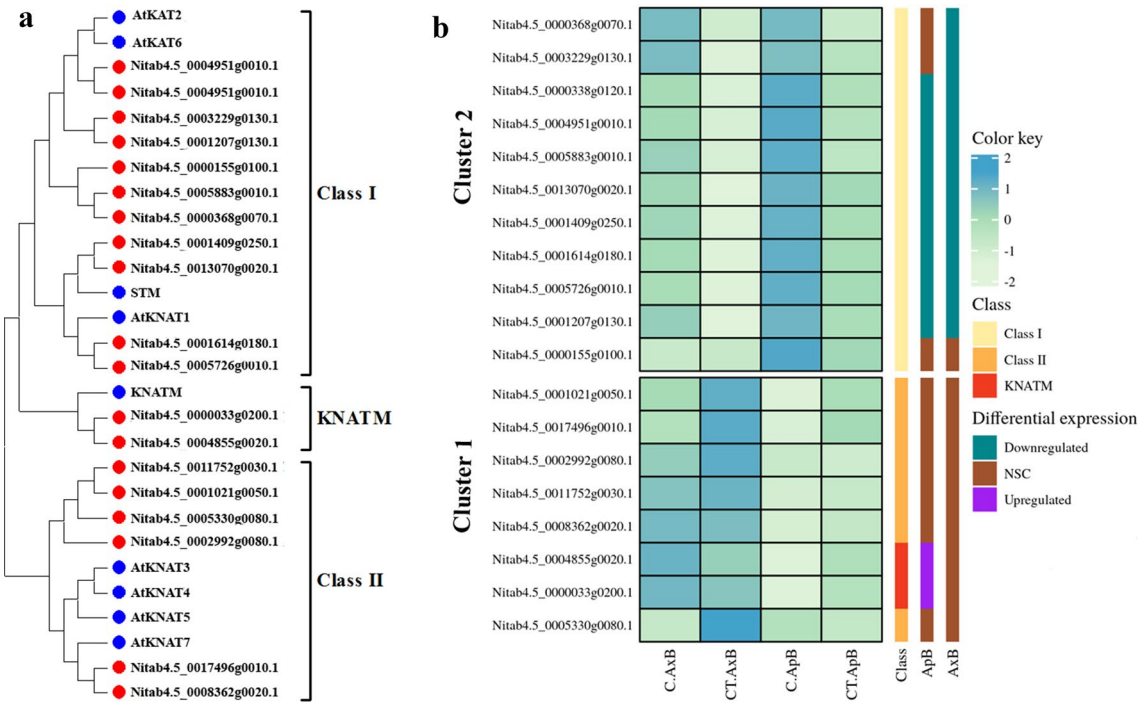

Fig. 4 Phylogenetic and gene expression analysis of KNOX gene family from tobacco. **a** A neighbor-joining phylogenetic tree of members of the *KNOX* gene family from *Arabidopsis thaliana* and *Nicotiana tabacum* (tobacco) was constructed using ClustalX and MEGA7.0 software with 1000 bootstraps. Nodes belonging to *A. thaliana* are represented by 'blue' circles while 'red' circles represent the genes from tobacco. **b** Heat map showing the FKPM values KNOX genes obtained by RNA-seq analysis. Rows represent probes and columns represent samples. The differential expression of each class of KNOX genes is annotated in the right bar. NSC, not significantly changed

A×B of tobacco (Table S7-8). RNA-seq analysis revealed that compared with the control, 20 and 57 genes related to phytohormone metabolism and signaling were significantly differentially expressed in CT-ApB (Table S7) and CT-AxB (Table S8), respectively. CT-A×B specific genes are related to SA, JA, GA and ET metabolism. Genes related to ET biosynthesis, including 1-amino-cyclopropane-1-carboxylate (ACC) synthase and ACC oxidase, were upregulated by MH-treatment in AxB. In addition, four DEGs related to ET biosynthesis were also common to CT-ApB and CT-AxB, which are downregulated in ApB but upregulated in AxB. These four DEGs are homologs of Arabidopsis 1-aminocyclopropane-1-carboxylic acid oxidase 4 (ACO4), a key gene in ET biosynthesis, indicating that MH treatment possibly induces ET accumulation leading to the suppression of bud growth. ET is known to inhibit cell division, DNA synthesis, and growth of AxB (Apelbaum and Burg 1972).

GAs play fundamental roles in plant growth and development. Three classes of enzymes, terpene synthases (TPSs), CYP450s and GA oxidases (GAoxs), are required for the biosynthesis of bioactive GAs from geranylgeranyl diphosphate (GGDP), and the pathway can be divided into two main steps. The early steps are catalyzed by a series of genes encoding enzymes, such as ent-copalyl diphosphate synthase (CPS), ent-kaurine synthase (KS), ent-kaurine oxidase (KO), and ENTKAURENOIC (KAO). The enzymes catalyzing later steps, including GA2 oxidase (GA2ox), GA20 oxidase (GA20ox), and GA3 oxidase (GA3ox), belong to the 2OG-Fe (II) oxygenase superfamily and are encoded by different gene families (Hedden and Phillips 2000). The genes involved in the later steps of GA biosynthesis are differentially regulated by developmental and environmental cues and play crucial but antagonistic roles in the accumulation of bioactive GA levels. For instance, upregulation of GA20ox and GA3ox increases the GA level, whereas higher expression of GA2ox decreases the GA level (Schomburg et al. 2003; Lo et al. 2008). GA is involved in A×B development in different plants including tomato, rice and aspen (Rinne et al. 2016; Martínez-Bello et al. 2015; Lo et al. 2008). In rice, GA negatively regulates the expression of two TFs, Homeobox 1 and TEOSINTE BRANCHED1 (TB1), which control meristem initiation and AxB outgrowth, respectively, and inhibits tillering (Lo et al. 2008). Two homologs of *Arabidopsis GA2ox* were upregulated in response to MH-treatment in our AxB dataset (Table S8), which possibly lowers the concentration of GA and inhibits AxB development.

MapMan visualization highlights the influence of MH treatment on different plant metabolic pathways

The pathway-based analysis was performed to associate biological functions with the genes differentially expressed in response to MH treatment. We used a comprehensive tool, the MapMan, to visualize the pathways affected by MH treatment in ApB and AxB tissues in tobacco. We overlaid the log2-fold change of DEGs to identify and visualize affected pathways. The number of genes in AxB affected by MH treatment was significantly higher compared to ApB, indicating a broader impact of MH on AxB. Genes related to defense such as secondary metabolites, proteolysis, pathogenesis-related genes and heat shock protein were downregulated in MH-treated ApB (Fig. 5a). However, unlike ApB, genes related to defense pathways and hormone biosynthesis were upregulated in AxB by MH treatment (Fig. 5b). In A×B, genes encoding enzymes in JA biosynthetic pathway, e.g. lipoxygenase and allene oxidase, were upregulated in response to MH treatment. Genes related to auxin homeostasis (IAA-amino acid hydrolase and GH3 family), ethylene biosynthesis and signaling ([ethylene response factor1 (ERF1), ERF2, ERF5, ERF4, 1-aminocyclopropane-1-carboxylate oxidase (ACOs) and 1-aminocyclopropane-1-carboxylate synthase (ACS)] were also induced by MH treatment in AxB. Plant glutathione S-transferases (GSTs) are a large gene family. There are 47 GST genes in *Arabidopsis thaliana*, 25 in *Glycine max*, and 42 in *Zea mays*. Based on sequence similarity, GSTs in plants are divided into three groups (I, II, and III) or, into six classes (tau, phi, zeta, theta, lambda, and DHAR). GSTs belong to *tau* and *phi* classes are more prevalent. The conjugation of toxic xenobiotics and oxidatively produced compounds to reduced glutathione is catalyzed by GSTs, which facilitates their metabolism, sequestration, or removal (Dalton et al. 2009). Expression of GSTs are also known to be induced by auxin and ethylene in plants including tobacco (van der Kop et al. 1996; Droog et al. 1995; Itzhaki and Woodson 1993; Van der Zaal et al. 1991). Unlike ApB, several homologs of auxin-responsive GSTs were found to be induced by MH treatment in A×B (Fig. 5b). Pathogenesis-related (PR) proteins play numerous roles in plant development and defense. The highly conserved plant PR proteins are classified into 17 classes based on amino acid sequence, serological relationship, and biological activities (Van Loon and Van Strien 1999). PR proteins are involved in plant immune responses (Stintzi et al. 1993) and enhance plant tolerance to both biotic and abiotic stresses (Wu et al. 2016). For instance, overexpression of PR proteins, such as *PR-1, PR-5,* or *PR-10*, enhances plant tolerance to a number of pathogens, such as *Rhizoctonia solani*, *Phytophthora nicotianae, Ralstonia solanacearum*, and *Pseudomonas syringae* (Datta et al. 1999; Sarowar et al. 2005). In addition, PR proteins have also been shown to play roles in adaption to abiotic stresses such as salt and heavy metal tolerance (Sarowar et al. 2005; de las Mercedes Dana et al. 2006). MH treatment induced the expression of several PR genes

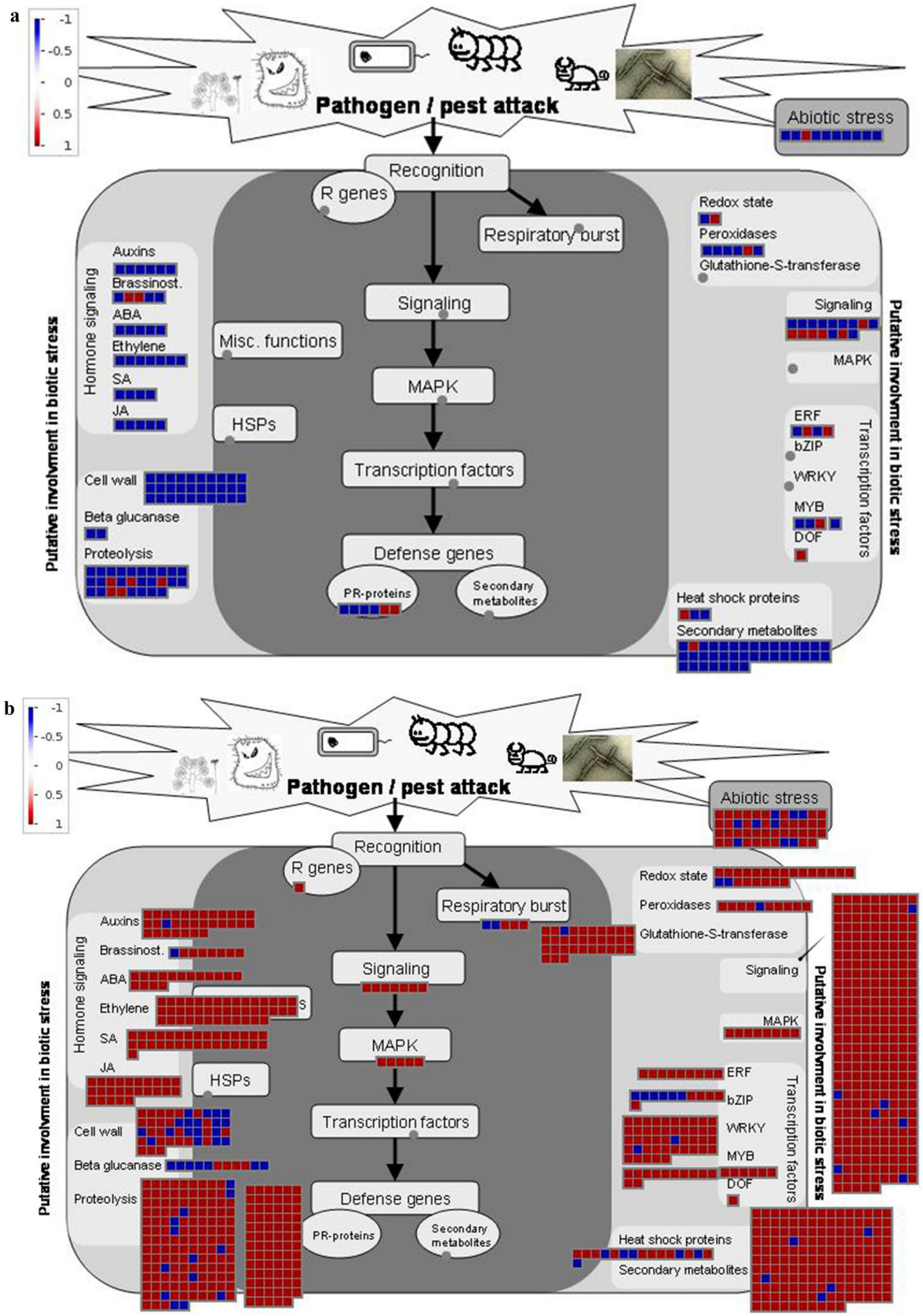
a
-1
-0.5
0
0.5
1
Pathogen / pest attack
Abiotic stress
Recognition
R genes
Respiratory burst
Signaling
Misc. functions
MAPK
HSPs
Transcription factors
Defense genes
PR-proteins
Secondary metabolites
Hormone signaling
Auxins
Brassinost.
ABA
Ethylene
SA
JA
Cell wall
Beta glucanase
Proteolysis
Redox state
Peroxidases
Glutathione-S-transferase
Signaling
MAPK
Transcription factors
ERF
bZIP
WRKY
MYB
DOF
Heat shock proteins
Secondary metabolites
Putative involvment in biotic stress
b
-1
-0.5
0
0.5
1
Pathogen / pest attack
Abiotic stress
Recognition
R genes
Respiratory burst
Signaling
MAPK
HSPs
Transcription factors
Defense genes
PR-proteins
Secondary metabolites
Hormone signaling
Auxins
Brassinost.
ABA
Ethylene
SA
JA
Cell wall
Beta glucanase
Proteolysis
Redox state
Peroxidases
Glutathione-S-transferase
Signaling
MAPK
Transcription factors
ERF
bZIP
WRKY
MYB
DOF
Heat shock proteins
Secondary metabolites
Putative involvment in biotic stress

◂**Fig. 5** MapMan visualization of differential gene expression in chemically topped apical bud and axillary bud compared with control. Each dot denotes a gene. 'Blue' color indicates downregulation while 'red' indicates upregulation. The log2-fold changes of significantly differentially expressed genes were imported and visualized in MapMan for the chemically topped apical bud sample with regard to pathogen/pest attack. **a** Chemically topped apical bud **b** chemically topped-axillary bud. The drawings in this figure are generated by MAPMAN (Thimm et al. 2004)

and secondary metabolite-related genes in AxB (Fig. 5b). Taken together, these results indicate that ApB and A×B respond differently to MH treatment (Fig. 5).

The promoters of MH-responsive genes are enriched in several known *cis*-acting elements

We identified several differentially expressed TF families in MH-treated AxB and ApB. We assumed that differentially expressed TFs are, at least in part, responsible for driving downstream changes in gene expression. We thus searched known plant *cis*-motifs, available in the JASPAR CORE and PLACE databases, which were overrepresented (*p value* < 0.05) in putative promoter regions (1 kb upstream from the translation start site) of DEGs with PSCAN and AME programs, respectively. The promoter analysis identified several putative TF-binding sites, such as MADS and HB family, in CT-ApB samples which corroborated with differentially expressed TF families (Table S9). Similarly, in CT-AxB, members of WRKY, bHLH, bZIP TF families were found to be abundant. These results provide initial clues into the TF-binding motifs that may be involved in regulating subsets of genes in response to MH treatment. Putative DEGs promoters were further scanned for the presence of motifs using the PLACE database. The MADS-box binding site (TTWCYAWWWWTRGWAA), DOF binding sites (AAAG, TAAAG, AAAAAGTAAAAAGTAAAA AAGTAAAAAG), and Sugar-responsive element (ACA TAAAATAAAAAAAGGCA) were enriched in CT-ApB downregulated genes (Table S10). AxB-downregulated genes were enriched in HB binding sites (CAATTATTA, TAATMATTA) and the sucrose-responsive element (AAT ACTAAT). Several *cis*-acting elements related to defense, including TGAC, TTGAC, TTGACY, TGACY, AAKAAT WYRTAWATAAAAMTTTTATWTA, MACGYGB, ACGTGKC, TTGACC, TGTGACATTGAAATTCTTTGACTTTA, AACGCGTGTC and AWTTCAAA, were enriched in CT-AxB upregulated genes. Moreover, several auxin-responsive elements (TATTTGCTTAA, TGACGTAA) and sucrose-responsive elements (AAAACTAAGAAAGACCGATGG AAAA, AATAGAAAA, and AATACTAAT) were also enriched in CT-AxB upregulated genes. We also identified several sucrose-responsive elements in the promoters of upregulated and downregulated genes in CT-ApB.

Validation of DEGs by real-time quantitative PCR

To validate the RNA-seq results, expression of ten differentially expressed genes involved in meristem development and phytohormone metabolism were analyzed by RT-qPCR. These genes encode the *KNOX* (*KNOX1* and *KNOX12*) genes, *AGL* (*AGL6* and *AGL20*) genes, *1-aminocyclopropane-1-carboxylate oxidase 4* (ACO4) and *salicylic acid carboxyl methyltransferase* (*SAMT*), *Gibberellin 20-oxidase* (GA20ox), IAA-leucine resistant-like 2 (ILL2), *Indole-3-acetic acid inducible 14* (*IAA14*), *GA-INSENSITIVE DWARF1B* (*GID1B*). The qRT-PCR results were consistent with the RNA-seq data, confirming the reliability and accuracy of our RNA-seq in this study (Fig. S3).

Discussion

MH exerts significant influence on tobacco transcriptome

Although MH is widely used in farming of tobacco and other crops for more than 70 years (Naylor 1950), the action of MH at molecular level is poorly understood. We believe that the gene expression profiles vary in ApB and A×B in response to MH treatment, requiring a refined analysis using separately isolated apical and axillary bud tissues. Here, we provide a comprehensive account on transcriptomic landscape of MH-treated ApB and A×B of tobacco. We generated 450 million clean reads from sequencing ApB and A×B RNA libraries, and, on an average, more than 75% of the total reads from control and MH-treated libraries were successfully mapped to the reference tobacco genome sequence, suggesting the good quality and depth of RNA-seq libraries (Table S2). The total number of transcripts in all analyzed samples varied from approximately 44,000 to 47,000, and approximately 10,000 mRNAs showed distinct accumulation patterns between MH-treated ApB and A×B (CT-ApB and CT-A×B) and control (C-ApB and C-A×B) (Fig. 1), indicating that MH elicits global changes in tobacco gene expression. In addition, MH has a broader effect on gene expression in A×B than ApB as the number of DEGs was significantly higher in MH-treated A×B compared to ApB (Fig. 2).

MH alters expression of genes involved in meristem development and cytokinin signaling

MH is known to suppress growth ApB and A×B growth in plants. We thus tried to identify and analyze expression of the genes involved in meristem development. GO enrichment analysis revealed that expression of the genes related to meristem development, cytokinin signaling and metabolism

are significantly affected (Fig. 3). Several TF families with known functions in meristem development were altered by MH treatment. Notably, TFs belonging to families of KNOX, MADS, and BTB/POZ domain were significantly affected. The KNOX genes are divided into two major subclasses (Gao et al. 2015). Class I KNOX genes, similar to maize *knotted1 (kn1)* gene, are predominantly expressed in the shoot apical meristem (SAM) (Gao et al. 2015; Hake et al. 2004). Class II KNOX genes exhibit diverse expression patterns (Gao et al. 2015). In *Arabidopsis*, the Class I KNOX gene, *shoot meristemless* (*STM*), has been shown to be a key player in shoot and floral meristem maintenance (Endrizzi et al. 1996). In addition, STM activates cytokinin (CK) biosynthetic genes and, consequently, increases CK accumulation (Yanai et al. 2005). Tobacco contains eleven class I KNOX genes, and MH-treatment repressed the expression of most class I KNOX genes, but not class II KNOX genes, in ApB and A×B (Fig. 4). MADS-box family genes regulate both flowering time and vegetative to reproductive phase transition in plants (Borner et al. 2000; Putterill et al. 2004). In MH-treated ApB, the expression of several MADS-box family TFs was downregulated (Fig. S2a). Notably affected MADS TF homologs included *SEP*, *PISTILLATA*, *AGAMOUS (AG)*, and *AP1*, that are well characterized for their roles in floral organ identity. In addition to KNOX and MADS, expression of genes belonging to BTB/POZ TF family with known functions in meristem development was affected by MH treatment. Collectively, our results suggest MH likely inhibits bud growth in two ways: (1) by suppressing the expression of key TFs in meristem development and (2) affecting CK biosynthesis through altering expression of STM-like KNOX TFs in tobacco.

CKs are implicated in nearly all aspects of plant growth and development, including cell division, apical dominance, leaf senescence, nutrient signaling, and shoot development (Hwang et al. 2012). The CK signaling pathway is a multistep His–Asp phosphorelay system that involves a sensor His-protein kinase (HK), His-containing phosphotransfer protein (HP) and response regulator (RR). The *Arabidopsis* response regulators (ARRs) are classified into three major groups based on phylogenetic analysis and domain structure: type-A ARRs, type-B ARRs, and the *Arabidopsis* pseudoresponse regulators (APRRs) (Hwang et al. 2002). Type-A ARRs are negative regulators (Hirose et al. 2007; Kiba et al. 2003), while type-B ARRs are positive regulators of CK signaling (Taniguchi et al. 2007; Yokoyama et al. 2007). The CK response factors (CRFs) are a group of related AP2/ERF TFs, which play a role in mediating part of the transcriptional response downstream of the CK signaling pathway. CRFs also induce the expression of type-A ARRs and suppress shoot growth (Raines et al. 2016). Our transcriptomic analysis revealed that expression of several Type-A ARRs and CRFs was upregulated in ApB following MH treatment. Taken together, our findings suggest that MH affects expression of key regulatory and CK signaling pathway genes to suppress bud growth in plants.

MH elicits defense response in tobacco

Our gene expression analysis revealed that MH elicits defense response in tobacco, evident by the upregulation of key genes regulated to oxylipin biosynthesis and secondary metabolism. WRKY TFs play key roles in plant defense and biosynthesis of secondary metabolites (Phukan et al. 2016; Schluttenhofer and Yuan 2015). Expression of at least 15 WRKY TFs, including WRKY28, WRKY33, WRKY50 and WRKY70, were upregulated in MH-treated AxB compared to control (Fig. 5). These WRKY TFs in *Arabidopsis* regulate defense response, phytohormone (JA and SA) signaling, and biosynthesis secondary metabolites (Chen et al. 2013; Li et al. 2004; Zheng et al. 2006). PR proteins play numerous roles in plant development and defense. Some PR proteins are involved in plant immune responses and plant tolerance to both biotic and abiotic stresses (Stintzi et al. 1993; Wu et al. 2016). Expression of several PR genes was altered in AxB following MH treatment. Collectively, our findings suggest that MH elicits defense response by activating expression of known regulatory genes in tobacco.

MH influences cell cycle, DNA replication, DNA damage and recombination

Previous studies have indicated that MH acts as an antimitotic agent (Clapp and Seltmann 1983), affecting axillary and apical bud growth by suppressing cell division in the actively growing tissues. Our gene expression analysis revealed that genes related to ORC, CDC, and MCM families, which are important for DNA replication, were downregulated in MH-treated A×B compared to the untreated control. In addition, MH treatment repressed the expression of BARD1 and RECQ helicase genes that are involved in DNA damage and recombination, potentially leading to inaccurate replication and ultimately cell viability (Table S3). These findings provide a possible mechanistic basis supporting the notion of MH being an antimitotic agent.

MH elicits similar as well as opposite responses in ApB and A×B

Differential gene expression and MAPMAN-based pathway analyses revealed that MH elicits both similar and opposite responses in tobacco ApB and A×B. For instance, altered expression of genes related to KNOX family TFs and cytokinin metabolism were common to both ApB and A×B (Fig. 2b). However, differential expression of several MADS TF genes was only found in ApB. This is possibly

due to the fact that tobacco naturally exhibits a strong apical dominance and suppresses the growth of A×B. The ApB is eventually transformed into floral meristem. MADS TFs play a critical role in vegetative to reproductive phase transition in plants. MH likely delays the phase transition by altering expression MADS TFs, which is interesting because previous observations have shown that MH application delays flowering (Naylor 1950). The other significant difference between ApB and A×B is the expression of genes related to defense response and secondary metabolism in A×B (Fig. 5). Many genes related to secondary metabolism, defense (e.g. pathogenesis-related (PR) genes and chitinase) and hormone (e.g. jasmonate) biosynthesis were upregulated in MH-treated A×B, but downregulated or not significantly affected in ApB. Previous studies have shown that manual topping induces defense response, JA signaling, and secondary metabolism in tobacco leaves; however, application of a local (*flumetralin*) or local–systemic (*fatty alcohols*) suckercide attenuates the induction (Singh et al. 2015). The current detailed study using ApB and A×B showed distinct effects of a systemic suckercide on the bud tissues.

cis-Regulatory motif enrichment in the MH-responsive gene promoters underscores the significant involvement of a subset of TF families

TF belonging to different families are known to interact with and bind specific *cis*-regulatory motifs present in the promoters to regulate gene expression. Therefore, *cis*-motifs provide important clues about the regulation of a metabolic or developmental pathway by a specific group of TFs. Selected *cis*-motifs have been used as baits to identify TFs that regulate a pathway. DNA binding motifs for several TF families, including bHLH, MYBs, MADS and WRKY, are well characterized. Our search for putative *cis*-regulatory motifs in the promoters of DEGs in ApB and AxB identified several potential MADS, WRKY, HB TF-binding elements (Tables S9 and 10). This information correlates well with the TFs differentially expressed in response to MH treatment and highlights the importance of a subset of TF families that are critical in MH-responsive gene expression in ApB and AxB.

Conclusion

Chemical topping is a method to reduce the labor requirement associated with crop production. Utilizing a chemical topping regime is a viable labor-saving alternative to reduce the overall cost without negatively impacting yield or leaf quality when compared to traditional manual topping practices. The adoption of chemical topping requires the application of MH prior to when manual topping would occur. Traditional practices would involve manually topping the tobacco and then applying MH. Instead of simply measuring how MH affecting vegetative tissues as a whole, we explored the influence of MH on gene expression in ApB and A×B of chemically topped burley tobacco. Our transcriptomic analysis revealed that MH has a significant influence on the gene expression in ApB and A×B. In both ApB and A×B, MH treatment affects expression of genes associated with meristem development, phytohormone metabolism, cell division, DNA repair, and recombination, which potentially leads to the inhibition of sucker development (Fig. 6) In addition, MH elicits plant defense responses by inducing the expression of genes involved in oxylipin biosynthesis, secondary metabolism, and defense. Furthermore, MH-treatment induces the expression of GST genes that are known to respond to various biotic and abiotic signals to protect plants from oxidative damage by detoxification and mitigation (Fig. 6). Both in traditional or chemical topping, accumulation of undesirable chemical residues on leaves as a result of suckercide application not only leads to pollution and potential health issues, but also affects the saleable value of tobacco leaves. Thus, development of a chemical-free sucker control system is highly desirable. The resulting information is a valuable resource for the identification and characterization of potential candidate genes for the development of suckercide-free tobacco in the future.

Author contribution statement L.Y., R.C.P., W.A.B., S.P. and S.K.S designed the research; S.K.S., M.D.R., X.H. and S.P. performed experiments; S.K.S. and S.P. analyzed data; and L.Y., S.K.S., S.P., M.D.R, W.A.B. and R.C.P. wrote the paper. All authors have read and approved the manuscript.

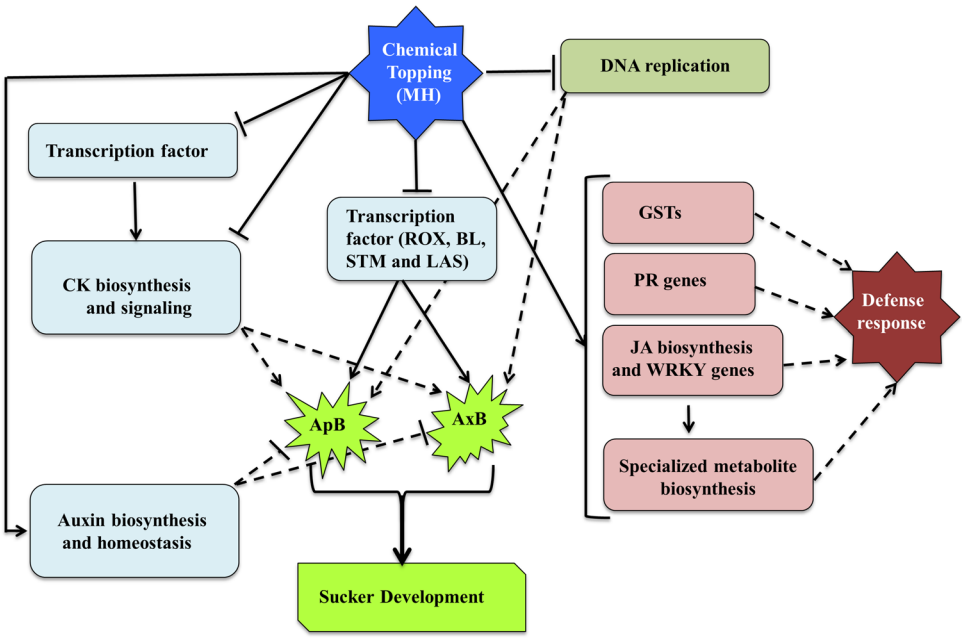

Fig. 6 A model depicting the effects of MH on different developmental and metabolic processes in tobacco. solid arrows represent positive regulation; solid T-bars represent negative regulation. Dashed arrow or T-bars represent possible regulation through combined effects of up- or down-regulated genes. *BL* Blind, *CK* cytokinin, *GST* Glutathione S-transferase, *JA* jasmonic acid, *LAS* Lateral suppressor, *MH* maleic hydrazide, *PR* genes Pathogenesis-related genes, *ROX* Regulator of axillary meristem formation, *STM* shoot meristemless

Acknowledgements This work is supported partially by grants from the Kentucky Tobacco Research and Development Center, University of Kentucky and The Council for Burley Tobacco, Kentucky, to L.Y. and S.P., and a Graduate Research Fellowship to M.D.R. from Department of Plant Soil Sciences, University of Kentucky.

Compliance with ethical standards

Conflict of interest The authors declare no conflicts of interest.

References

Apelbaum A, Burg SP (1972) Effect of ethylene on cell division and deoxyribonucleic acid synthesis in *Pisum sativum*. Plant Physiol 50(1):117–124

Backman TWH, Girke T (2016) systemPipeR: NGS workflow and report generation environment. BMC Bioinformatics 17(1):388

Bäurle I, Dean C (2006) The timing of developmental transitions in plants. Cell 125(4):655–664

Borner R, Kampmann G, Chandler J, Gleißner R, Wisman E, Apel K, Melzer S (2000) A MADS domain gene involved in the transition to flowering in Arabidopsis. Plant J 24(5):591–599

Boss PK, Bastow RM, Mylne JS, Dean C (2004) Multiple pathways in the decision to flower: enabling, promoting, and resetting. Plant Cell 16(suppl 1):S18–S31

Chen X, Liu J, Lin G, Wang A, Wang Z, Lu G (2013) Overexpression of AtWRKY28 and AtWRKY75 in Arabidopsis enhances resistance to oxalic acid and Sclerotinia sclerotiorum. Plant Cell Rep 32(10):1589–1599

Clapp MK, Seltmann H (1983) Anatomy of axillary meristems from tobacco plants treated with maleic hydrazide. Bot Gaz 144(1):86–91

Cline JA, Bakker CJ (2016) Prohexadione-calcium, ethephon, trinexapac-ethyl, and maleic hydrazide reduce extension shoot growth of apple. Canad J Plant Sci 97(3):457–465

Collins W, Hawks S (1993) Principles of flue-cured tobacco production. Collins-Hawks Books, Raleigh

Dalton DA, Boniface C, Turner Z, Lindahl A, Kim HJ, Jelinek L, Govindarajulu M, Finger RE, Taylor CG (2009) Physiological roles of glutathione *s*-transferases in soybean root nodules. Plant Physiol 150(1):521–530

Datta K, Velazhahan R, Oliva N, Ona I, Mew T, Khush G, Muthukrishnan S, Datta S (1999) Over-expression of the cloned rice thaumatin-like protein (PR-5) gene in transgenic rice plants enhances environmental friendly resistance to Rhizoctonia solani causing sheath blight disease. Theor Appl Genet 98(6–7):1138–1145

de las Mercedes Dana M, Pintor-Toro JA, Cubero B (2006) Transgenic tobacco plants overexpressing chitinases of fungal origin show enhanced resistance to biotic and abiotic stress agents. Plant Physiol 142 (2):722–730

Ditta G, Pinyopich A, Robles P, Pelaz S, Yanofsky MF (2004) The SEP4 gene of *Arabidopsis thaliana* functions in floral organ and meristem identity. Curr Biol 14(21):1935–1940

Droog F, Spek A, van der Kooy A, de Ruyter A, Hoge H, Libbenga K, Hooykaas P, van der Zaal B (1995) Promoter analysis of the auxin-regulated tobacco glutathione S-transferase genes Nt103-1 and Nt103-35. Plant Mol Biol 29(3):413–429

Endrizzi K, Moussian B, Haecker A, Levin JZ, Laux T (1996) The shoot meristemless gene is required for maintenance of undifferentiated cells in Arabidopsis shoot and floral meristems and acts at a different regulatory level than the meristem genes WUSCHEL and ZWILLE. Plant J 10(6):967–979

Fisher LR, Priest JA (2004) Topping and sucker management and use of ethephon. Flue-Cured Tobacco Information, North Carolina State University:106–130

Galperin MY, Rigden DJ, Fernandez-Suarez XM (2015) The 2015 nucleic acids research database issue and molecular biology database collection. Nucleic Acids Res 43:D1–D5

Gao J, Yang X, Zhao W, Lang T, Samuelsson T (2015) Evolution, diversification, and expression of KNOX proteins in plants. Front Plant Sci 6:882

Gao Q-M, Venugopal S, Navarre D, Kachroo A (2011) Low oleic acid-derived repression of jasmonic acid-inducible defense responses

requires the WRKY50 and WRKY51 proteins. Plant Physiol 155(1):464–476
Gianfagna T, Logendra L, Durner E, Janes H (1997) Improving tomato harvest index by controlling crop height and side shoot production. Life Support Biosph Sci 5(2):255–261
Goldshmidt A, Alvarez JP, Bowman JL, Eshed Y (2008) Signals derived from YABBY gene activities in organ primordia regulate growth and partitioning of Arabidopsis shoot apical meristems. Plant Cell 20(5):1217–1230
Gu Z, Eils R, Schlesner M (2016) Complex heatmaps reveal patterns and correlations in multidimensional genomic data. Bioinformatics 32:2847–2849
Guo H, Kan Y, Liu W (2011) Differential expression of miRNAs in response to topping in flue-cured tobacco (*Nicotiana tabacum*) roots. PLoS ONE 6(12):e28565
Gutierrez C (2009) The arabidopsis cell division cycle. The Arabidopsis Book / American Society of Plant Biologists 7:e0120
Hake S, Smith HMS, Holtan H, Magnani E, Mele G, Ramirez J (2004) The role of knox genes in plant development. Annu Rev Cell Deve Biol 20(1):125–151
Hartmann U, Höhmann S, Nettesheim K, Wisman E, Saedler H, Huijser P (2000) Molecular cloning of SVP: a negative regulator of the floral transition in Arabidopsis. Plant J 21(4):351–360
Hedden P, Phillips AL (2000) Gibberellin metabolism: new insights revealed by the genes. Trends Plant Sci 5(12):523–530
Higo K, Ugawa Y, Iwamoto M, Korenaga T (1999) Plant cis-acting regulatory DNA elements (PLACE) database: 1999. Nucleic Acids Res 27(1):297–300
Hirose N, Makita N, Kojima M, Kamada-Nobusada T, Sakakibara H (2007) Overexpression of a Type-a response regulator alters rice morphology and cytokinin metabolism. Plant Cell Physiol 48(3):523–539
Huang X, Effgen S, Meyer RC, Theres K, Koornneef M (2012) Epistatic natural allelic variation reveals a function of AGAMOUS-like6 in axillary bud formation in arabidopsis. Plant Cell 24(6):2364–2379
Huerta-Cepas J, Szklarczyk D, Forslund K, Cook H, Heller D, Walter MC, Rattei T, Mende DR, Sunagawa S, Kuhn M, Jensen LJ, von Mering C, Bork P (2016) eggNOG 4.5: a hierarchical orthology framework with improved functional annotations for eukaryotic, prokaryotic and viral sequences. Nucleic Acids Res 44(D1):D286–D293
Hwang I, Chen H-C, Sheen J (2002) Two-component signal transduction pathways in arabidopsis. Plant Physiol 129(2):500–515
Hwang I, Sheen J, Müller B (2012) Cytokinin signaling networks. Annu Rev Plant Biol 63(1):353–380
Itzhaki H, Woodson WR (1993) Characterization of an ethylene-responsive glutathione S-transferase gene cluster in carnation. Plant Mol Biol 22(1):43–58
Khan A, Fornes O, Stigliani A, Gheorghe M, Castro-Mondragon JA, van der Lee R, Bessy A, Chèneby J, Kulkarni SR, Tan G, Baranasic D, Arenillas DJ, Sandelin A, Vandepoele K, Lenhard B, Ballester B, Wasserman WW, Parcy F, Mathelier A (2018) JASPAR 2018: update of the open-access database of transcription factor binding profiles and its web framework. Nucleic Acids Res 46(D1):D260–D266
Khan M, Ragni L, Tabb P, Salasini BC, Chatfield S, Datla R, Lock J, Kuai X, Despres C, Proveniers M, Yongguo C, Xiang D, Morin H, Rulliere JP, Citerne S, Hepworth SR, Pautot V (2015) Repression of lateral organ boundary genes by pennywise and poundfoolish is essential for meristem maintenance and flowering in arabidopsis. Plant Physiol 169(3):2166–2186
Kiba T, Yamada H, Sato S, Kato T, Tabata S, Yamashino T, Mizuno T (2003) The type-A response regulator, ARR15, acts as a negative regulator in the cytokinin-mediated signal transduction in Arabidopsis thaliana. Plant Cell Physiol 44(8):868–874
Klein WH, Leopold AC (1953) The effects of maleic hydrazide on flower initiation. Plant Physiol 28(2):293–298
Koo SC, Bracko O, Park MS, Schwab R, Chun HJ, Park KM, Seo JS, Grbic V, Balasubramanian S, Schmid M, Godard F, Yun DJ, Lee SY, Cho MJ, Weigel D, Kim MC (2010) Control of lateral organ development and flowering time by the Arabidopsis thaliana MADS-box Gene AGAMOUS-LIKE6. Plant J 62(5):807–816
Langmead B, Salzberg SL (2012) Fast gapped-read alignment with Bowtie 2. Nat Meth 9(4):357–359
Lario LD, Ramirez-Parra E, Gutierrez C, Spampinato CP, Casati P (2013) Anti-silencing function1 proteins are involved in ultraviolet-induced DNA damage repair and are cell cycle regulated by E2F transcription factors in Arabidopsis. Plant Physiol 162(2):1164–1177
Lee JH, Yoo SJ, Park SH, Hwang I, Lee JS, Ahn JH (2007) Role of SVP in the control of flowering time by ambient temperature in Arabidopsis. Genes Dev 21(4):397–402
Leibfried A, To JP, Busch W, Stehling S, Kehle A, Demar M, Kieber JJ, Lohmann JU (2005) WUSCHEL controls meristem function by direct regulation of cytokinin-inducible response regulators. Nature 438(7071):1172–1175
Li J, Brader G, Palva ET (2004) The WRKY70 transcription factor: a node of convergence for jasmonate-mediated and salicylate-mediated signals in plant defense. Plant Cell 16(2):319–331
Li W, Tian Z, Yu D (2015) WRKY13 acts in stem development in Arabidopsis thaliana. Plant Sci 236:205–213
Li W, Wang H, Yu D (2016) Arabidopsis WRKY transcription factors WRKY12 and WRKY13 oppositely regulate flowering under short-day conditions. Mol Plant 9(11):1492–1503
Liu S, Bartnikas LM, Volko SM, Ausubel FM, Tang D (2016) Mutation of the glucosinolate biosynthesis enzyme cytochrome P450 83A1 monooxygenase increases camalexin accumulation and powdery mildew resistance. Front Plant Sci 7:227
Lo S-F, Yang S-Y, Chen K-T, Hsing Y-I, Zeevaart JAD, Chen L-J, Yu S-M (2008) A novel class of gibberellin 2-oxidases control semidwarfism, tillering, and root development in rice. Plant Cell 20(10):2603–2618
Logendra LS, Gianfagna TJ, Janes HW (2004) Preventing side shoot development with C8/C10 fatty acids increases yield and reduces pruning time in greenhouse tomato. Hort Sci 39(7):1652–1654
Love MI, Huber W, Anders S (2014) Moderated estimation of fold change and dispersion for RNA-seq data with DESeq2. Genome Biol 15(12):550
Maere S, Heymans K, Kuiper M (2005) BiNGO: a Cytoscape plugin to assess overrepresentation of gene ontology categories in Biological Networks. Bioinformatics 21(16):3448–3449
Magnani E, Hake S (2008) KNOX Lost the OX: The arabidopsis KNATM gene defines a novel class of KNOX transcriptional regulators missing the homeodomain. Plant Cell 20(4):875–887
Marie AI, Ihsan A, Salih SH (2007) Effect of sowing date, topping and some growth regulators on growth, pod and seeds yield of okra (Abelmoschus esculentus L.M.). In: African crop science society conference proceedings, vol 8, pp 473–478
Martínez-Bello L, Moritz T, López-Díaz I (2015) Silencing C(19)-GA 2-oxidases induces parthenocarpic development and inhibits lateral branching in tomato plants. J Exp Bot 66(19):5897–5910
McLeay RC, Bailey TL (2010) Motif Enrichment Analysis: a unified framework and an evaluation on ChIP data. BMC Bioinform 11(1):165
Mitchell A, Chang H-Y, Daugherty L, Fraser M, Hunter S, Lopez R, McAnulla C, McMenamin C, Nuka G, Pesseat S, Sangrador-Vegas A, Scheremetjew M, Rato C, Yong S-Y, Bateman A, Punta M, Attwood TK, Sigrist CJA, Redaschi N, Rivoire C, Xenarios I, Kahn D, Guyot D, Bork P, Letunic I, Gough J, Oates M, Haft D, Huang H, Natale DA, Wu CH, Orengo C, Sillitoe I, Mi H,

Thomas PD, Finn RD (2015) The InterPro protein families database: the classification resource after 15 years. Nucleic Acids Res 43(D1):D213–D221

Müller D, Schmitz G, Theres K (2006) Blind homologous R2R3 Myb genes control the pattern of lateral meristem initiation in arabidopsis. Plant Cell 18(3):586–597

Muñoz-Viana R, Wildhaber T, Trejo-Arellano MS, Mozgová I, Hennig L (2017) Arabidopsis chromatin assembly factor 1 is required for occupancy and position of a subset of nucleosomes. Plant J 92(3):363–374

Naylor AW (1950) Observations on the effects of maleic hydrazide on flowering of tobacco, maize and cocklebur. Proc Natl Acad Sci USA 36(4):230–232

Oh SA, Bourdon V, Dickinson HG, Twell D, Park SK (2014) Arabidopsis Fused kinase TWO-IN-ONE dominantly inhibits male meiotic cytokinesis. Plant Reprod 27(1):7–17

Pattanaik S, Kong Q, Zaitlin D, Werkman JR, Xie CH, Patra B, Yuan L (2010) Isolation and functional characterization of a floral tissue-specific R2R3 MYB regulator from tobacco. Planta 231(5):1061–1076

Peek D (1995) Chemical topping burley tobacco. Theses and Dissertations, University of Kentucky

Phukan UJ, Jeena GS, Shukla RK (2016) WRKY Transcription factors: molecular regulation and stress responses in plants. Front Plant Sci 7:760

Prasad KVSK, Abdel-Hameed AAE, Xing D, Reddy ASN (2016) Global gene expression analysis using RNA-seq uncovered a new role for SR1/CAMTA3 transcription factor in salt stress. Sci Rep 6:27021

Putterill J, Laurie R, Macknight R (2004) It's time to flower: the genetic control of flowering time. BioEssays 26(4):363–373

Qi Y, Guo H, Li K, Liu W (2012) Comprehensive analysis of differential genes and miRNA profiles for discovery of topping-responsive genes in flue-cured tobacco roots. FEBS J 279(6):1054–1070

R Core Team (2020) R: A language and environment for statistical computing. R Foundation for Statistical Computing, Vienna, Austria

Raines T, Shanks C, Cheng C-Y, McPherson D, Argueso CT, Kim HJ, Franco-Zorrilla JM, López-Vidriero I, Solano R, Vaňková R, Schaller GE, Kieber JJ (2016) The cytokinin response factors modulate root and shoot growth and promote leaf senescence in Arabidopsis. Plant J 85(1):134–147

Rao KN, Bangarayya M, Murthy YCN, Babu DP (2003) Effect of topping at different growth stages on the yield and quality of fcv tobacco grown in northern light soils of Andhra Pradesh Indian. J Plant Physiol 8(1):48–52

Renou A, Téréta I, Togola M (2011) Manual topping decreases bollworm infestations in cotton cultivation in Mali. Crop Protection 30(10):1370–1375

Richmond MD (2018) Chemical topping burley tobacco. Theses and Dissertations, University of Kentucky

Rijpkema AS, Vandenbussche M, Koes R, Heijmans K, Gerats T (2010) Variations on a theme: Changes in the floral ABCs in angiosperms. Semin Cell Dev Biol 21(1):100–107

Rinne PLH, Paul LK, Vahala J, Kangasjärvi J, van der Schoot C (2016) Axillary buds are dwarfed shoots that tightly regulate GA pathway and GA-inducible 1,3-β-glucanase genes during branching in hybrid aspen. J Exp Bot 67:5975–5991

Sarowar S, Kim YJ, Kim EN, Kim KD, Hwang BK, Islam R, Shin JS (2005) Overexpression of a pepper basic pathogenesis-related protein 1 gene in tobacco plants enhances resistance to heavy metal and pathogen stresses. Plant Cell Rep 24(4):216–224

Schluttenhofer C, Yuan L (2015) Regulation of specialized metabolism by WRKY transcription factors. Plant Physiol 167(2):295–306

Schmieder R, Edwards R (2011) Quality control and preprocessing of metagenomic datasets. Bioinformatics 27(6):863–864

Schomburg FM, Bizzell CM, Lee DJ, Zeevaart JAD, Amasino RM (2003) Overexpression of a novel class of gibberellin 2-oxidases decreases gibberellin levels and creates dwarf plants. Plant Cell 15(1):151–163

Shannon P, Markiel A, Ozier O, Baliga NS, Wang JT, Ramage D, Amin N, Schwikowski B, Ideker T (2003) Cytoscape: a software environment for integrated models of biomolecular interaction networks. Genome Res 13(11):2498–2504

Singh F, Kumar R, Kumar P, Pal S (2011) Effect of irrigation, fertility and topping on Indian mustard (*Brassica juncea*). Progress Agricul 11(2):477–478

Singh SK, Wu Y, Ghosh JS, Pattanaik S, Fisher C, Wang Y, Lawson D, Yuan L (2015) RNA-sequencing reveals global transcriptomic changes in *Nicotiana tabacum* responding to topping and treatment of axillary-shoot control chemicals. Sci Rep 5:18148

Smalle J, Kurepa J, Yang P, Babiychuk E, Kushnir S, Durski A, Vierstra RD (2002) Cytokinin growth responses in arabidopsis involve the 26S proteasome subunit RPN12. Plant Cell 14(1):17–32

Stintzi A, Heitz T, Prasad V, Wiedemann-Merdinoglu S, Kauffmann S, Geoffroy P, Legrand M, Fritig B (1993) Plant 'pathogenesis-related' proteins and their role in defense against pathogens. Biochimie 75(8):687–706

Supek F, Bošnjak M, Škunca N, Šmuc T (2011) REVIGO summarizes and visualizes long lists of gene ontology terms. PLoS ONE 6(7):e21800

Tang S, Wang Y, Li Z, Gui Y, Xiao B, Xie J, Zhu Q-H, Fan L (2012) Identification of wounding and topping responsive small RNAs in tobacco (*Nicotiana tabacum*). BMC Plant Biol 12(1):28

Taniguchi M, Sasaki N, Tsuge T, Aoyama T, Oka A (2007) ARR1 directly activates cytokinin response genes that encode proteins with diverse regulatory functions. Plant Cell Physiol 48(2):263–277

Tavakol E, Okagaki R, Verderio G, Shariati JV, Hussien A, Bilgic H, Scanlon MJ, Todt NR, Close TJ, Druka A, Waugh R, Steuernagel B, Ariyadasa R, Himmelbach A, Stein N, Muehlbauer GJ, Rossini L (2015) The Barley *Uniculme4* Gene Encodes a BLADE-ON-PETIOLE-Like Protein That Controls Tillering and Leaf Patterning. Plant Physiol 168(1):164–174

Thimm O, Blasing O, Gibon Y, Nagel A, Meyer S, Kruger P, Selbig J, Muller LA, Rhee SY, Stitt M (2004) MAPMAN: a user-driven tool to display genomics data sets onto diagrams of metabolic pathways and other biological processes. Plant J 37(6):914–939

Tripathi M, Chaudhary B, Singh S, Bh H (2013) Growth and yield of sunnhemp (Crotalaria juncea L.) as influenced by spacing and topping practices. African J Agric Res 8(28):3744–3749

Tso T-C (1990) Production, physiology, and biochemistry of tobacco plant. Ideals, USA

van der Kop DA, Schuyer M, Scheres B, van der Zaal BJ, Hooykaas PJ (1996) Isolation and characterization of an auxin-inducible glutathione S-transferase gene of Arabidopsis thaliana. Plant Molecular Biol 30(4):839–844

Van der Zaal E, Droog F, Boot C, Hensgens L, Hoge J, Schilperoort R, Libbenga K (1991) Promoters of auxin-induced genes from tobacco can lead to auxin-inducible and root tip-specific expression. Plant Mol Biol 16(6):983–998

Van Loon LC, Van Strien EA (1999) The families of pathogenesis-related proteins, their activities, and comparative analysis of PR-1 type proteins. Physiol Mol Plant Pathol 55(2):85–97

Vasudevan S, Sudarshan J, Kurdikeri M, Dharmatti P (2008) Influence of pinching of apical bud and chemical sprays on seed yield and quality of fenugreek. Karnataka J Agric Sci 21:26–29

Venezian A, Dor E, Achdari G, Plakhine D, Smirnov E, Hershenhorn J (2017) The Influence of the Plant Growth Regulator Maleic Hydrazide on Egyptian Broomrape Early Developmental Stages

and Its Control Efficacy in Tomato under Greenhouse and Field Conditions. Front Plant Sci 8:691

Wu J, Kim SG, Kang KY, Kim J-G, Park S-R, Gupta R, Kim YH, Wang Y, Kim ST (2016) Overexpression of a pathogenesis-related protein 10 enhances biotic and abiotic stress tolerance in rice. Plant Pathology J 32(6):552–562

Xu M, Hu T, McKim SM, Murmu J, Haughn GW, Hepworth SR (2010) Arabidopsis BLADE-ON-PETIOLE1 and 2 promote floral meristem fate and determinacy in a previously undefined pathway targeting APETALA1 and AGAMOUS-LIKE24. Plant J 63(6):974–989

Yanai O, Shani E, Dolezal K, Tarkowski P, Sablowski R, Sandberg G, Samach A, Ori N (2005) Arabidopsis KNOXI proteins activate cytokinin biosynthesis. Curr Biol 15(17):1566–1571

Yang F, Wang Q, Schmitz G, Müller D, Theres K (2012a) The bHLH protein ROX acts in concert with RAX1 and LAS to modulate axillary meristem formation in Arabidopsis. Plant J 71(1):61–70

Yang M, Jiao Y (2016) Regulation of axillary meristem initiation by transcription factors and plant hormones. Front Plant Sci 7:183

Yang Y, Ouyand Z, Wang S-f (2012b) The study on the cotton growth and development under two different agronomy practices topping and pruning via without topping and pruning. Acta Agric Bor Sin 27:234–239

Yokoyama A, Yamashino T, Amano Y, Tajima Y, Imamura A, Sakakibara H, Mizuno T (2007) Type-B ARR transcription factors, ARR10 and ARR12, are implicated in cytokinin-mediated regulation of protoxylem differentiation in roots of Arabidopsis thaliana. Plant Cell Physiol 48(1):84–96

Zambelli F, Pesole G, Pavesi G (2009) Pscan: finding over-represented transcription factor binding site motifs in sequences from co-regulated or co-expressed genes. Nucleic Acids Res 37(Suppl_2):247–252

Zheng Z, Qamar SA, Chen Z, Mengiste T (2006) Arabidopsis WRKY33 transcription factor is required for resistance to necrotrophic fungal pathogens. Plant J 48(4):592–605

toxins

MDPI

Article

Rumen and Serum Metabolomes in Response to Endophyte-Infected Tall Fescue Seed and Isoflavone Supplementation in Beef Steers

Taylor B. Ault-Seay [1], Emily A. Melchior-Tiffany [1,†], Brooke A. Clemmons [1,‡], Juan F. Cordero [1], Gary E. Bates [2], Michael D. Flythe [3], James L. Klotz [3], Huihua Ji [4], Jack P. Goodman [5], Kyle J. McLean [1] and Phillip R. Myer [1,*]

1 Department of Animal Science, University of Tennessee, Knoxville, TN 37996, USA; tault1@vols.utk.edu (T.B.A.-S.); eam@nmsu.edu (E.A.M.-T.); Brooke.Clemmons@tamuc.edu (B.A.C.); Juan.Cordero@utk.edu (J.F.C.); kmclea10@utk.edu (K.J.M.)
2 Department of Plant Sciences, University of Tennessee, Knoxville, TN 37996, USA; gbates@utk.edu
3 USDA-ARS, Forage-Animal Production Research Unit, Lexington, KY 40546, USA; michael.flythe@ars.usda.gov (M.D.F.); James.Klotz@ars.usda.gov (J.L.K.)
4 Kentucky Tobacco Research and Development Center, University of Kentucky, Lexington, KY 40546, USA; hji4@email.uky.edu
5 Department of Plant and Soil Sciences, University of Kentucky, Lexington, KY 40546, USA; jpgood2@email.uky.edu
* Correspondence: pmyer@utk.edu; Tel.: +1-865-974-3184
† Current Address: Department of Animal and Range Sciences, New Mexico State University, Las Cruces, NM 88003, USA.
‡ Current Address: Department of Agriculture, Texas A&M University-Commerce, Commerce, TX 75428, USA.

Received: 4 November 2020; Accepted: 24 November 2020; Published: 26 November 2020

Abstract: Fescue toxicosis impacts beef cattle production via reductions in weight gain and muscle development. Isoflavone supplementation has displayed potential for mitigating these effects. The objective of the current study was to evaluate isoflavone supplementation with fescue seed consumption on rumen and serum metabolomes. Angus steers (n = 36) were allocated randomly in a 2 × 2 factorial arrangement of treatments including endophyte-infected (E+) or endophyte-free (E−) tall fescue seed, with (P+) or without (P−) isoflavones. Steers were provided a basal diet with fescue seed for 21 days, while isoflavones were orally administered daily. Following the trial, blood and rumen fluid were collected for metabolite analysis. Metabolites were extracted and then analyzed by UPLC-MS. The MAVEN program was implemented to identify metabolites for MetaboAnalyst 4.0 and SAS 9.4 statistical analysis. Seven differentially abundant metabolites were identified in serum by isoflavone treatment, and eleven metabolites in the rumen due to seed type ($p < 0.05$). Pathways affected by treatments were related to amino acid and nucleic acid metabolism in both rumen fluid and serum ($p < 0.05$). Therefore, metabolism was altered by fescue seed in the rumen; however, isoflavones altered metabolism systemically to potentially mitigate detrimental effects of seed and improve animal performance.

Keywords: beef cattle; endophyte; ergot alkaloid; fescue toxicosis; isoflavone; metabolites

Key Contribution: As fescue toxicosis causes multiple symptoms that negatively impact beef cattle performance, isoflavone consumption may reduce these effects. The current study found tall fescue seed type to mainly impact the rumen metabolome, while isoflavone supplementation affected the host metabolome in the serum, potentially improving animal growth and development during fescue toxicosis.

1. Introduction

Tall fescue is the major forage used to feed cattle in pasture-based systems of the southeast and covers approximately 14 million hectares across the United States [1]. The advantage of tall fescue is hardiness of the plants attributed to the presence of a fungal endophyte (*Epichloë coenophialum*, formerly known as *Neotyphodium coenophialum* and *Acremonium coenophialum*) living in a mutualistic relationship with the plant [2]. However, the endophyte produces ergot alkaloids that are toxic to animals that consume them for an extended period of time [3]. Ergot alkaloids are able to bind biogenic amine receptors on blood vessels, resulting in vasoconstriction throughout the body [4–6]. This results in a condition known as fescue toxicosis, which is commonly observed by the animal's inability to thermoregulate [7], poor reproductive performance [1], and reduced average daily gain [8], significantly reducing overall animal performance. Therefore, researchers are tasked with identifying management methods and therapeutics to alleviate these consequences to cattle producers.

Pasture management methods have been evaluated for reducing the impact of fescue toxicosis in cattle. Inter-seeding of legumes, such as red clover, to mitigate the effects of fescue toxicosis has proved beneficial in cattle grazing endophyte-infected tall fescue [9]. Recent research has found phytoestrogenic compounds, known as isoflavones, present in red clover may be responsible for reducing the effects of fescue toxicosis. Isoflavones act as an agonist on the β-adrenergic receptors present on blood vessels to promote vasodilation [10], reversing the effects of ergot alkaloid induced vasoconstriction. Additionally, isoflavones act as a natural antibiotic selective against hyper-ammonia-producing bacteria (HAB) and some cellulolytic and amylolytic bacteria [11,12]. The reduction of ammonia levels as a result of less HAB in the rumen allows more amino acids to be absorbed and used by the ruminant, while altered celluloytic and amylolytic bacteria can influence the production of volatile fatty acids for energy. Therefore, the increase in blood flow and altered rumen fermentation may improve nutrient delivery and utilization for host metabolic processes contributing to animal growth.

The objective of the present study is to evaluate the effect of isoflavone supplementation with tall fescue seed consumption on beef steer's rumen and serum metabolomes. Ruminal and circulating metabolites may provide insights into altered bacterial and host metabolic functions that improve steer performance on endophyte infected tall fescue with the administration of isoflavones.

2. Results

2.1. Global Rumen Fluid and Serum Metabolome Comparison

An orthogonal partial least squares discriminant analysis (O-PLS-DA) was used to depict the relationship between the global rumen and serum metabolomes, which illustrated distinct separation between the two metabolomes (Figure 1). A heatmap was also used to visualize the top 25 rumen fluid and serum metabolites by individual steer (Figure 2). The heatmap supports that there is very little similarity between the overall ruminal and circulating metabolites.

2.2. Rumen Fluid Metabolome

All identified rumen fluid metabolites are presented in Supplementary File 1 with means and standard errors of the mean by treatment combination group. To visualize the effect between steers of the E+P+ and E−P− groups on the rumen fluid metabolome, a partial least squares discriminant analysis (PLS-DA) was created and a significant distinct overlap among seed type was noted (Figure 3). Correlation analyses were performed to analyze the correlation of individual rumen metabolites with the treatment combination groups, and variable importance in the projection (VIP) scores were generated to determine the metabolites that contributed to variation in rumen fluid metabolomes among treatment combination groups. Xylose was negatively correlated with the treatments ($r = -0.57$) and had one of the greatest impacts on metabolome differences among all treatments ($p = 0.01$) (Figure 4, Table 1). Individual metabolite and metabolic pathway analyses were not significantly impacted by the interaction of seed type and isoflavone treatments ($p > 0.05$).

The rumen metabolome was analyzed by the main effects of seed type and isoflavone treatment. In order to visualize the difference in rumen fluid metabolomes, an O-PLS-DA was generated for the main effects of seed type (Figure 5A) and isoflavone treatment (Figure 5B). For seed type and isoflavone treatment, partial separation was observed between endophyte-infected and endophyte-free seed (Figure 5A). Additionally, partial separation was observed between steers receiving isoflavones and those that did not receive isoflavones (Figure 5B). Correlation analysis indicated hypoxanthine was negatively correlated (r = −0.56) and determined by VIP analysis to have a significant impact on the rumen fluid metabolome differences between endophyte-infected and endophyte-free seed treatments ($p = 0.01$; Figure 6A; Table 1). For isoflavone treatments, trehalose/sucrose was positively correlated (r = 0.06), but had no impact on the rumen fluid metabolome differences (Figure 6B). Metabolites that differed by seed type are presented in Table 1. Eleven metabolites differed significantly as a result of endophyte-infected versus endophyte-free treatments ($p < 0.05$, Table 1). No individual metabolite differences were observed in the rumen fluid as a result of isoflavone treatment. Metabolic pathways that differed significantly by seed type or isoflavone treatment are presented in Table 2. Twenty metabolic pathways were affected by seed type, but only two pathways were affected by isoflavones ($p < 0.05$).

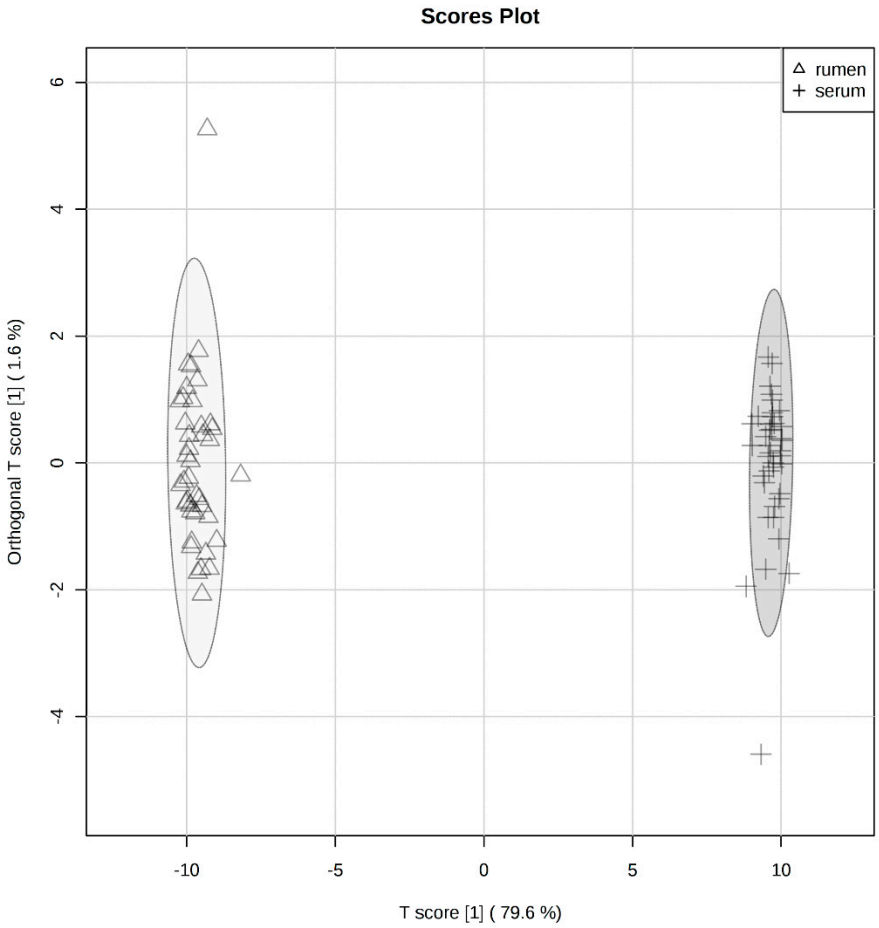

Figure 1. Orthogonal partial least squares discriminant analysis (O-PLS-DA) visualizing separation of rumen fluid (triangle) and serum (plus-sign) metabolomes. Ellipse represents a 95% confidence interval.

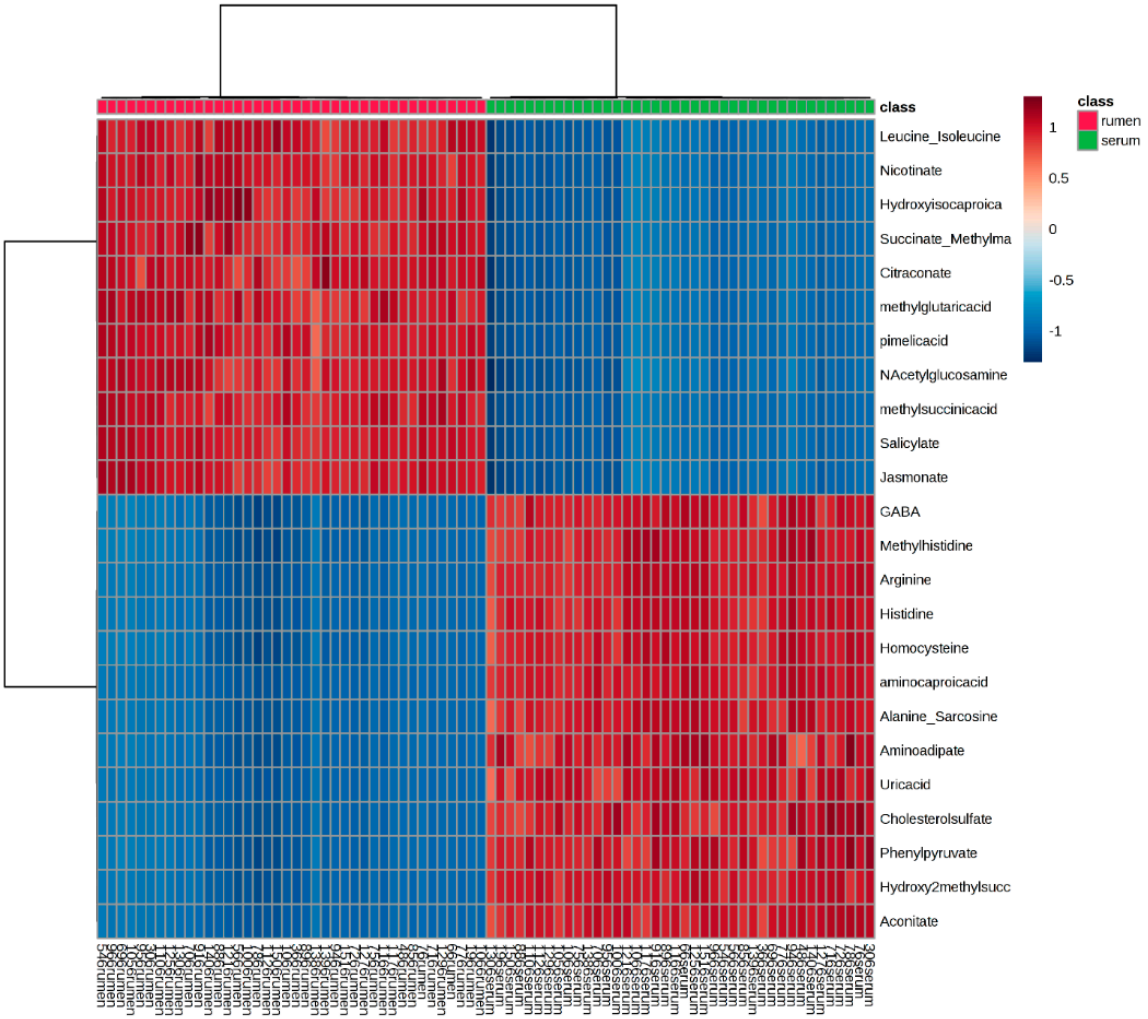

Figure 2. Heatmap of top 25 metabolites of rumen fluid and serum metabolomes by individual steers. Rumen fluid is represented by the red square at the top of the heatmap and serum metabolites are represented by the green squares.

Table 1. Rumen fluid metabolites that significantly differed by seed type.

Metabolite	Seed Type †		*p* Value €
	E+	E−	
Dihydroxybenzoate	$5.90 \times 10^7 \pm 5.35 \times 10^6$ B	$8.43 \times 10^7 \pm 6.26 \times 10^6$ A	0.05
Adenine *	$2.30 \times 10^7 \pm 1.13 \times 10^7$ B	$6.84 \times 10^7 \pm 1.32 \times 10^7$ A	0.02
CMP *	$9.17 \times 10^5 \pm 7.64 \times 10^5$ B	$3.17 \times 10^6 \pm 8.95 \times 10^5$ A	0.04
Deoxyuridine *	$8.04 \times 10^5 \pm 2.71 \times 10^5$ B	$1.74 \times 10^6 \pm 3.18 \times 10^5$ A	0.02
Glutamate *	$7.18 \times 10^7 \pm 2.17 \times 10^7$ B	$1.57 \times 10^8 \pm 2.54 \times 10^7$ A	0.05
Guanosine *	$3.00 \times 10^5 \pm 1.44 \times 10^5$ B	$8.63 \times 10^5 \pm 1.69 \times 10^5$ A	0.05
Homoserine/threonine	$1.02 \times 10^7 \pm 8.90 \times 10^5$ B	$6.65 \times 10^6 \pm 7.60 \times 10^5$ A	0.05
Hypoxanthine *	$4.40 \times 10^7 \pm 1.66 \times 10^7$ B	$1.17 \times 10^8 \pm 1.94 \times 10^7$ A	0.01
Uracil *	$5.76 \times 10^7 \pm 1.19 \times 10^7$ B	$1.08 \times 10^8 \pm 1.39 \times 10^7$ A	0.02
Xanthine *	$1.79 \times 10^8 \pm 4.34 \times 10^7$ B	$3.48 \times 10^8 \pm 5.09 \times 10^7$ A	0.01
Xylose *	$3.63 \times 10^6 \pm 1.05 \times 10^6$ B	$8.69 \times 10^6 \pm 1.23 \times 10^6$ A	0.01

* Analysis based on ranked data; † values are measured as mean ± SEM of area under the peak; € significance determined at $p \leq 0.05$ based on FDR-corrected *p*-values; AB within-row represent groupings based on Fisher's LSD.

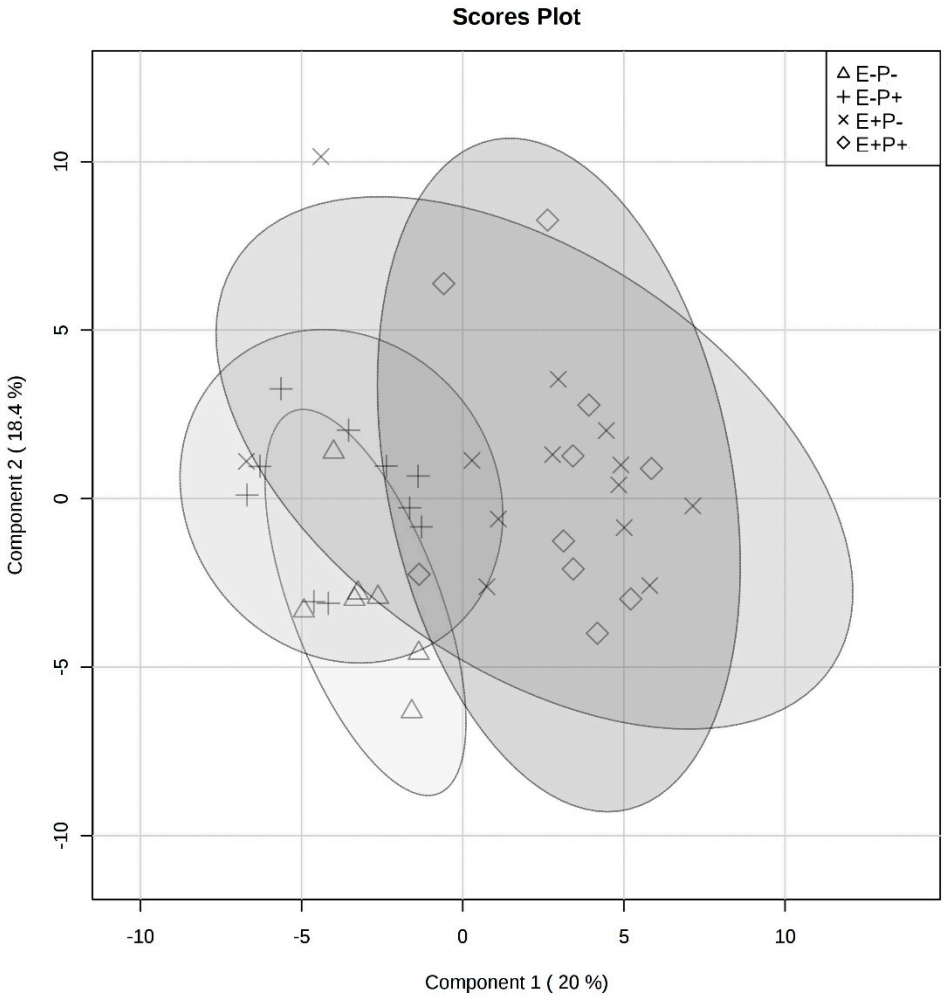

Figure 3. Partial least squares discriminant analysis (PLS-DA) visualizing differences in rumen fluid metabolomes between endophyte-free seed without isoflavones (triangle), endophyte-free with isoflavones (plus-sign), endophyte-infected without isoflavones (multiplication-sign), and endophyte-infected with isoflavones (diamond) treatment groups. Ellipse represents a 95% confidence interval.

Table 2. Rumen fluid metabolic pathways impacted by seed type or isoflavone treatments.

Pathway	FDR	Impact	*p* Value
Seed Type			
Purine metabolism	2.73×10^{-4}	0.338	6.89×10^{-6}
Arginine and proline metabolism	2.73×10^{-4}	0.075	1.07×10^{-5}
Pentose and glucuronate interconversions	3.42×10^{-4}	0	2.01×10^{-5}
Beta-Alanine metabolism	3.69×10^{-4}	0	2.89×10^{-5}
Pyrimidine metabolism	3.99×10^{-4}	0.494	5.92×10^{-5}
Pantothenate and CoA biosynthesis	3.99×10^{-4}	0.229	6.7×10^{-5}
Aminoacyl-tRNA biosynthesis	3.99×10^{-4}	0.2	7.81×10^{-5}
Tyrosine metabolism	3.99×10^{-4}	0	7.83×10^{-5}
Novobiocin biosynthesis	3.99×10^{-4}	0	7.83×10^{-5}
Thiamine metabolism	3.99×10^{-4}	0	7.83×10^{-5}
Phenylalanine metabolism	7.94×10^{-4}	0.001	1.71×10^{-4}

Table 2. *Cont.*

Pathway	FDR	Impact	*p* Value
Phenylalanine, tyrosine, and tryptophan biosynthesis	0.001	4.60×10^{-4}	2.78×10^{-4}
Carbapenem biosynthesis	0.001	0	3.25×10^{-4}
Butanoate metabolism	0.001	0	3.25×10^{-4}
Porphyrin and chlorophyll metabolism	0.001	0	3.25×10^{-4}
Pentose phosphate pathway	0.003	0.07	0.001
Amino sugar and nucleotide sugar metabolism	0.004	0.109	0.001
Glutathione metabolism	0.004	0.014	0.002
D-Glutamine and D-glutamate metabolism	0.004	0.172	0.002
Nitrogen metabolism	0.004	0	0.002
Isoflavone Treatment			
Methane metabolism	0.84824	0.154	0.032
Sulfur metabolism	0.84824	0	0.033

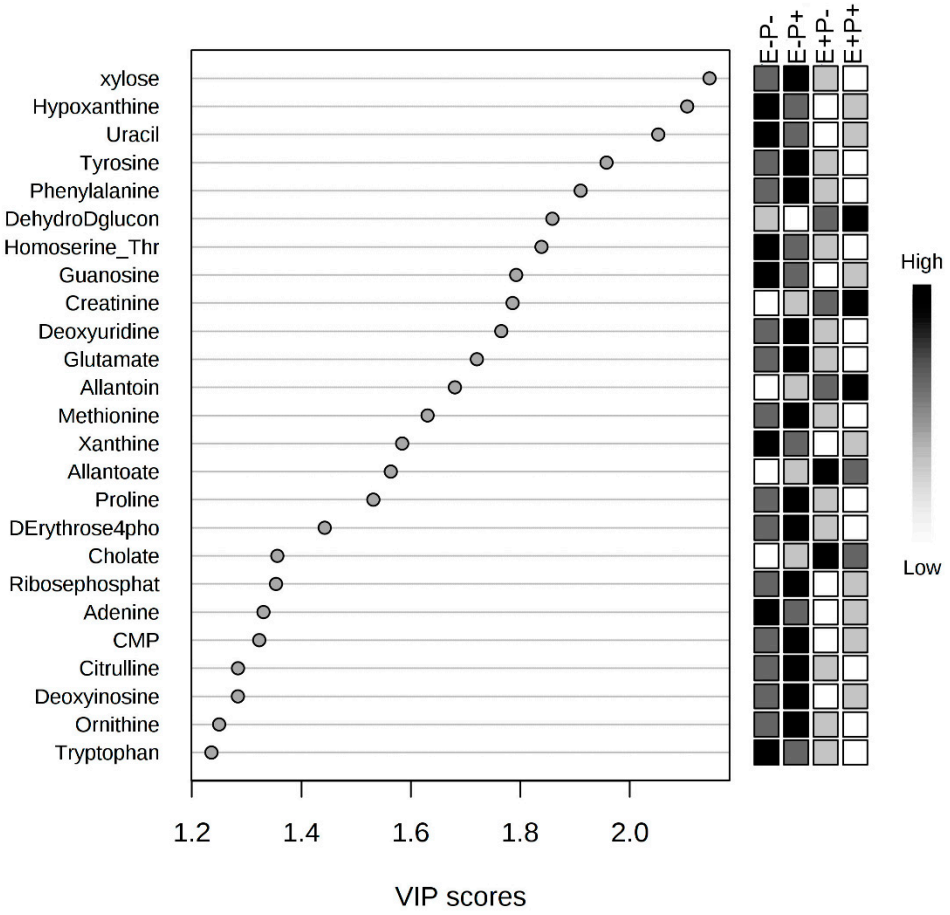

Figure 4. Variable importance in the projection (VIP) plot indicates xylose to have the greatest influence on the differences in rumen fluid metabolomes between all treatment groups.

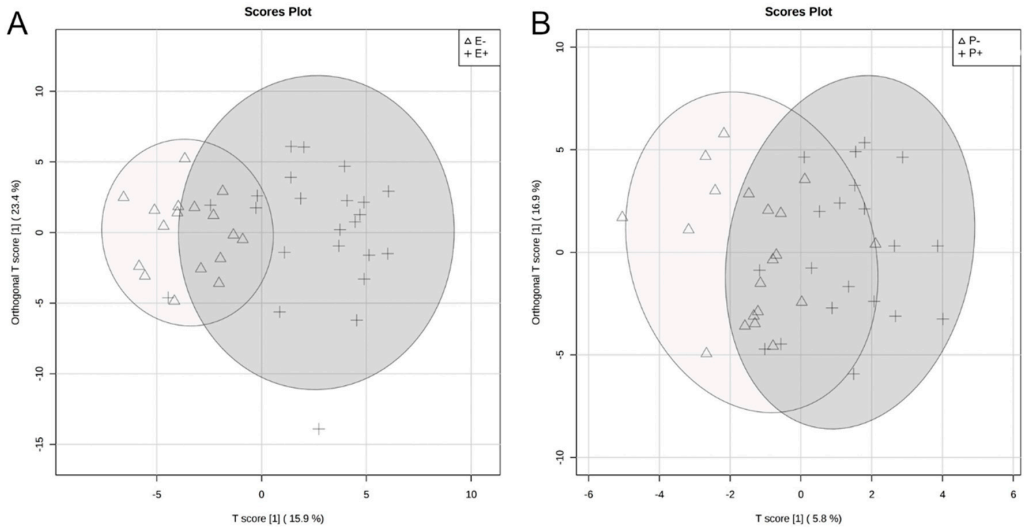

Figure 5. Orthogonal partial least squares discriminant analyses (O-PLS-DA) visualizing differences in rumen fluid metabolomes by seed type (**A**) and isoflavone (**B**) treatments. For seed type (**A**), endophyte-free (E−) steers are represented by a triangle and endophyte-infected (E+) steers by a plus-sign. For isoflavone treatments (**B**), steers receiving isoflavones (P+) are represented by a plus-sign and without isoflavones (P−) by a triangle. Ellipse represents a 95% confidence interval.

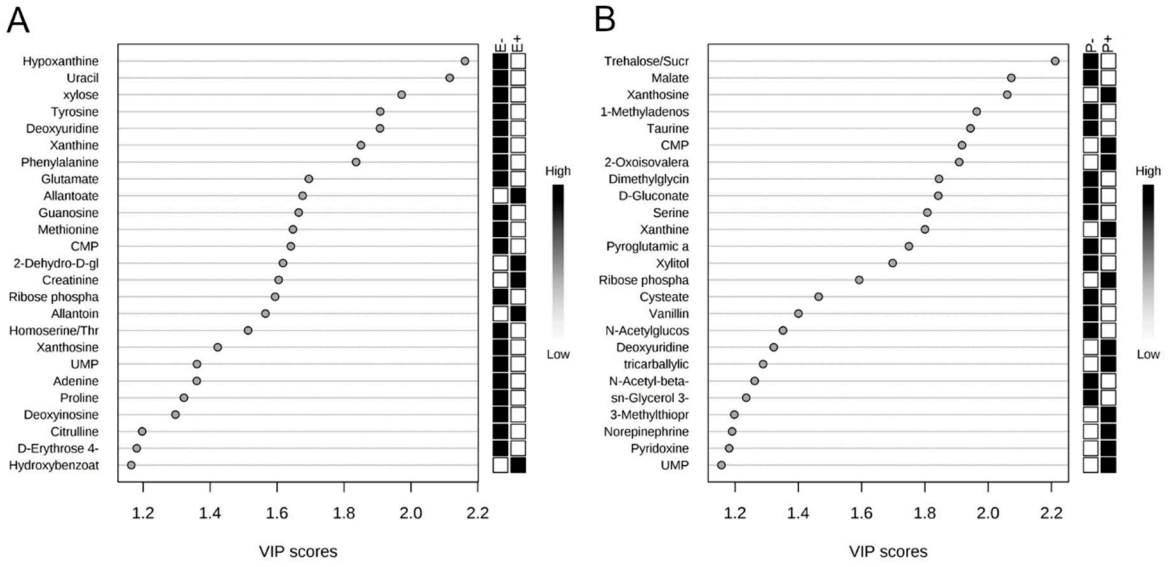

Figure 6. Variable importance in the projection (VIP) plots indicate hypoxanthine to have the greatest influence on the differences in rumen fluid metabolomes between endophyte-free (E−) and endophyte-infected (E+) seed treatment groups (**A**), and trehalose sucrose to have the greatest influence between isoflavone treated (P+) and control (P−) groups (**B**).

2.3. Serum Metabolome

All identified serum metabolites are presented in Supplementary File 2 with means and standard errors of the mean by treatment combination group. The serum metabolome was first analyzed by treatment combination group, isoflavone × seed type. The PLS-DA analysis indicated significant overlap among groups, with partial separation between the E+P+ and E−P− groups (Figure 7). Correlation analyses were performed to determine the correlation of individual serum metabolites with the treatment combination groups and VIP were generated to determine the metabolites that contributed to variation in serum metabolomes among treatment combination groups. Pantothenate

was negatively correlated with interaction of seed type × isoflavone treatments (r = −0.29) and had the largest impact on metabolome differences, although not significant (p = 0.07; Figure 8).

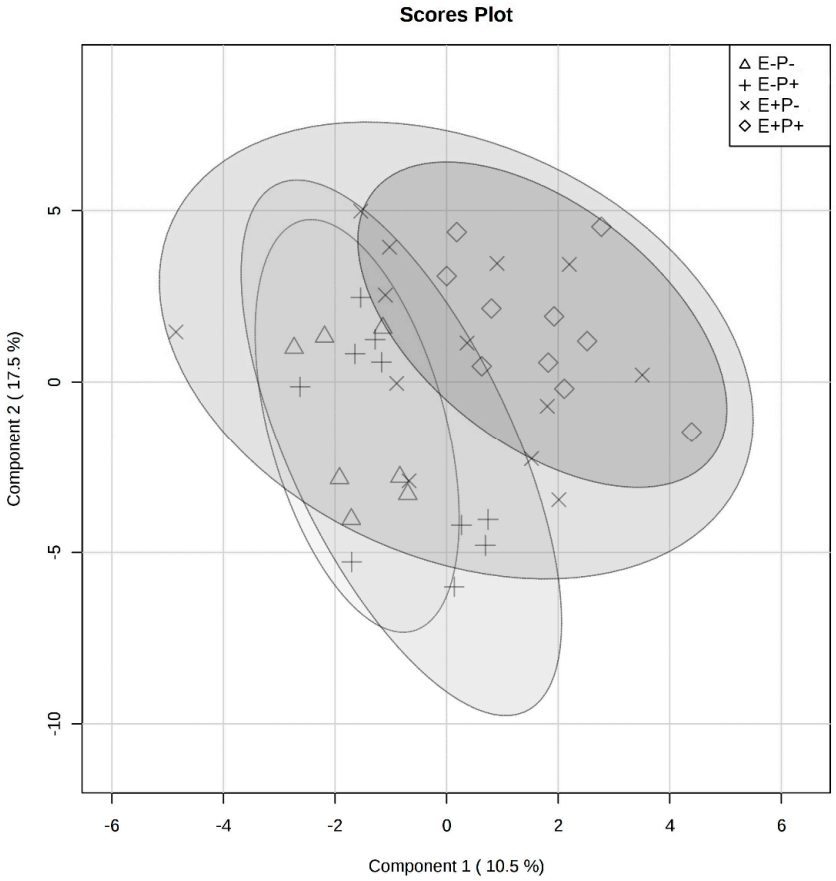

Figure 7. Partial least squares discriminant analysis (PLS-DA) visualizing differences in serum metabolomes between all treatment groups: endophyte-free seed without isoflavones (triangle), endophyte-free with isoflavones (plus-sign), endophyte-infected without isoflavones (multiplication-sign), and endophyte-infected with isoflavones (diamond). Ellipse represents a 95% confidence interval.

Similar to rumen fluid, no individual serum metabolites or metabolic pathways were affected by the interaction of seed type and isoflavone treatment ($p > 0.05$). The serum metabolome was then analyzed by the main effects of seed type or isoflavone treatment. In order to visualize the difference in serum metabolomes, O-PLS-DA analyses were generated for seed type (Figure 9A) and isoflavone treatment (Figure 9B). For seed type, partial separation was observed between E+ and E− seed groups (Figure 9A). However, complete separation of serum metabolomes was illustrated between steers receiving isoflavones and those that did not receive isoflavones (Figure 9B). Correlation analysis indicated AMP was negatively correlated with seed treatment (r = −0.35) and determined by VIP analysis to have the greatest impact on serum metabolome differences between E+ and E− steers (p = 0.03; Figure 10A). Between isoflavone treatment groups, citrulline was positively correlated (r = 0.47) and had the greatest impact on serum metabolome differences (p = 0.003; Figure 10B). Seven metabolites differed significantly as a result of isoflavone treatment ($p < 0.05$, Table 3), while no metabolites differed as a result of seed type ($p > 0.05$). Thirteen metabolic pathways differed ($p < 0.05$) as a result of seed type including glyoxylate and dicarboxylate metabolism; arginine biosynthesis; and alanine, aspartate, and glutamate metabolism ($p < 0.01$; Table 4). For isoflavone treatments, eight metabolic pathways were affected ($p < 0.05$), including pyrimidine metabolism and arginine and proline metabolism ($p < 0.01$; Table 4).

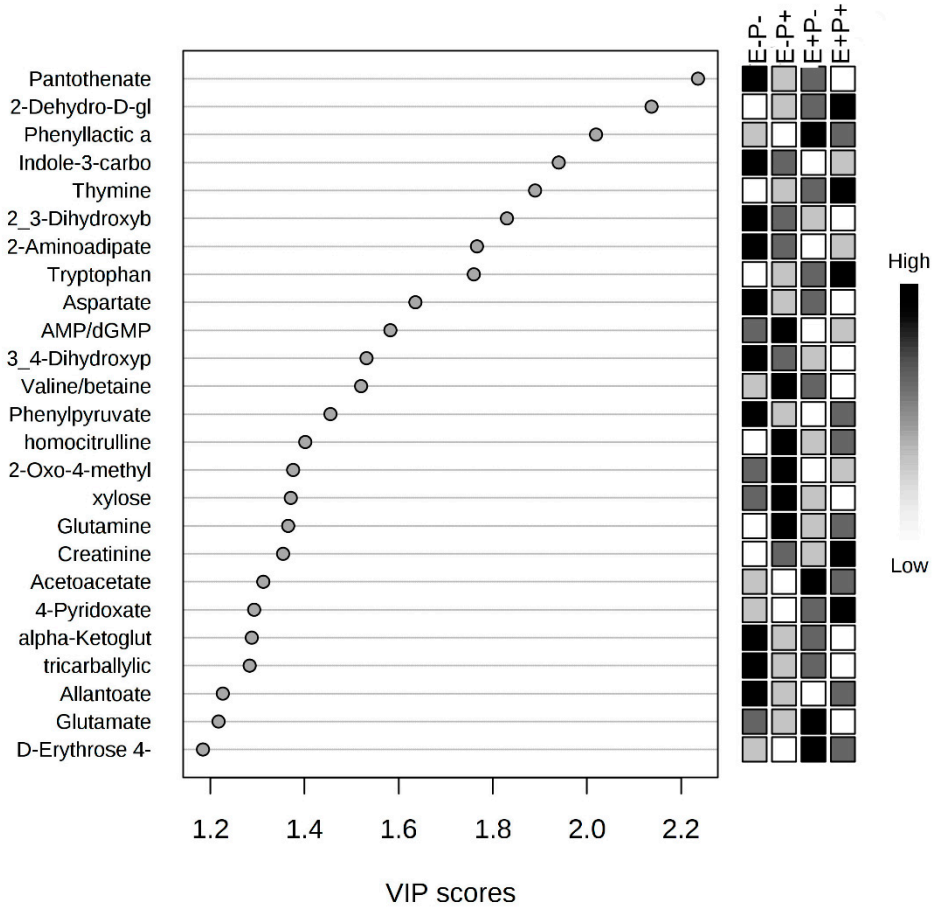

Figure 8. Variable importance in the projection (VIP) plot indicates pantothenate to have the greatest influence on the differences in serum metabolomes between all treatment groups.

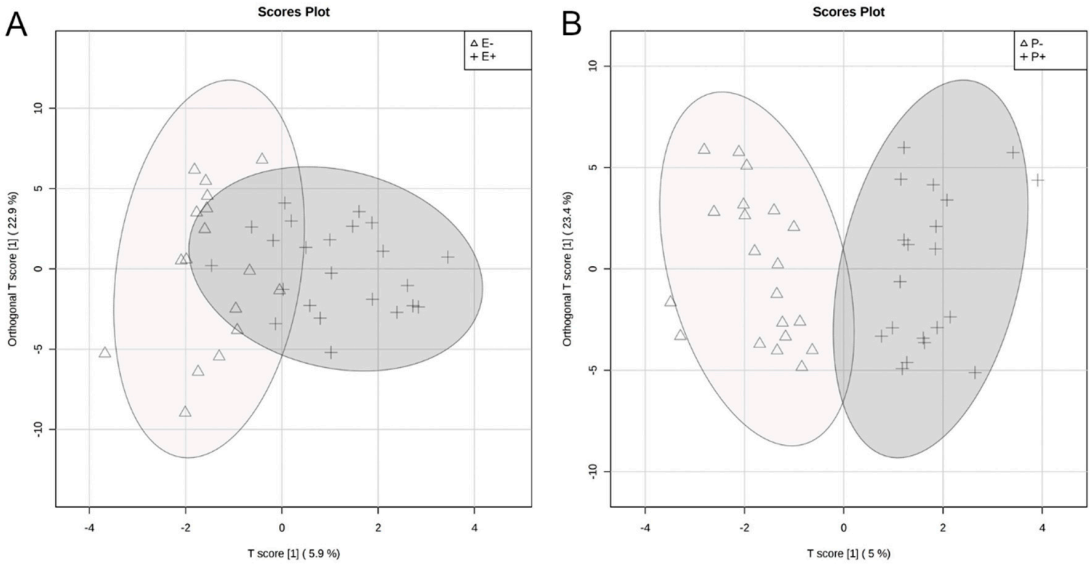

Figure 9. Orthogonal partial least squares discriminant analyses (O-PLS-DA) visualizing differences in serum metabolomes by seed type (**A**) and isoflavone (**B**) treatments. For seed type (**A**), endophyte-free (E−) steers are represented by a triangle and endophyte-infected (E+) steers by a plus-sign. For isoflavone treatments (**B**), steers receiving isoflavones (P+) are represented by a plus-sign and without isoflavones (P−) by a triangle. Ellipse represents a 95% confidence interval.

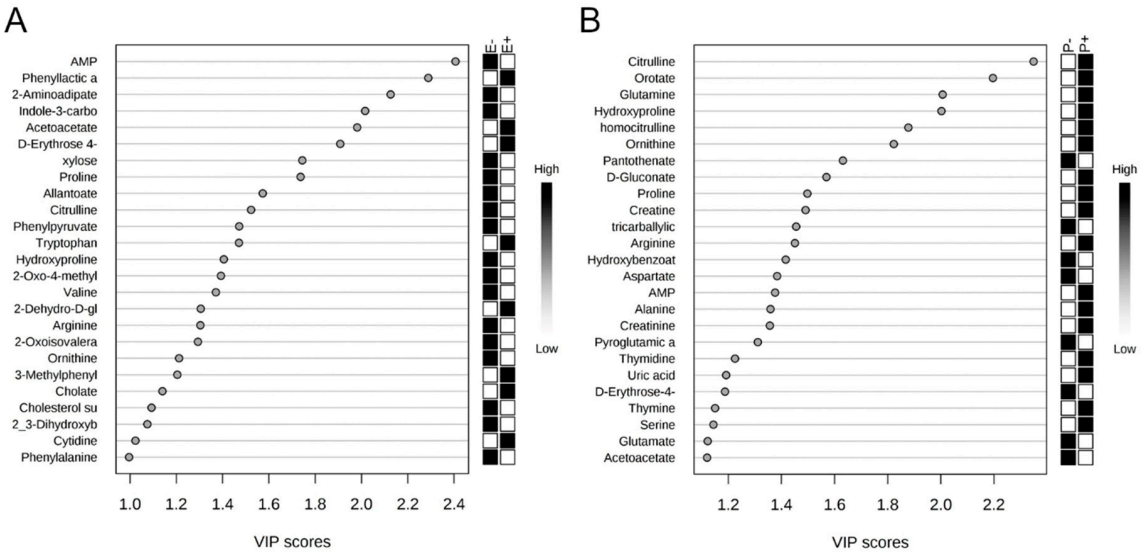

Figure 10. Variable importance in the projection (VIP) plot indicates AMP to have the greatest influence on the differences in serum metabolomes between endophyte-free (E−) and endophyte-infected (E+) seed treatment groups (**A**), and citrulline to have the greatest influence between isoflavone treated (P+) and control (P−) groups (**B**).

Table 3. Individual serum metabolites that significantly differed by isoflavone treatment.

Metabolite	Isoflavone Treatment †		*p* Value €
	P+	P−	
Histidine *	$8.50 \times 10^6 \pm 8.94 \times 10^5$	$1.05 \times 10^7 \pm 9.37 \times 10^5$	0.05
Cytidine *	$1.51 \times 10^6 \pm 4.89 \times 10^5$ B	$2.67 \times 10^7 \pm 5.12 \times 10^5$ A	0.01
Pantothenate	$6.64 \times 10^6 \pm 1.84 \times 10^6$ B	$1.51 \times 10^7 \pm 1.93 \times 10^6$ A	0.01
Homocysteine	$1.47 \times 10^6 \pm 1.28 \times 10^5$ B	$2.02 \times 10^6 \pm 1.35 \times 10^5$ A	0.02
Allantoin	$1.94 \times 10^8 \pm 1.14 \times 10^7$ B	$2.37 \times 10^8 \pm 1.19 \times 10^7$ A	0.03
GABA	$9.68 \times 10^5 \pm 1.40 \times 10^5$ B	$1.41 \times 10^6 \pm 1.44 \times 10^5$ A	0.05
Methylhistidine	$8.35 \times 10^5 \pm 6.25 \times 10^4$	$1.04 \times 10^6 \pm 6.51 \times 10^4$	0.05

* Analysis based on ranked data; † values are measured as mean ± SEM of area under the peak; € significance determined at $p \leq 0.05$ based on FDR-corrected *p*-values; AB within-row represent groupings based on Fisher's LSD.

Table 4. Serum metabolic pathways affected by seed type and isoflavone treatments.

Pathway	FDR	Impact	*p* Value
Seed Type			
Glyoxylate and dicarboxylate metabolism	0.013	0.11	0.005
Arginine biosynthesis	0.013	0.51	0.006
Alanine, aspartate, and glutamate metabolism	0.015	0.73	0.007
Cysteine and methionine metabolism	0.051	0.14	0.024
Glycine, serine, and threonine metabolism	0.054	0.16	0.029
Ubiquinone and other terpenoid-quinone biosynthesis	0.054	0	0.029
Aminobenzoate degradation	0.054	0	0.029
Vitamin B6 metabolism	0.069	0.05	0.039
Monobactam biosynthesis	0.069	0	0.041
Lysine biosynthesis	0.069	0	0.041
Nicotinate and nicotinamide metabolism	0.069	0.06	0.042
Tryptophan metabolism	0.07	0	0.044
Cyanoamino acid metabolism	0.076	0	0.05

Table 4. *Cont.*

Pathway	FDR	Impact	*p* Value
Isoflavone Treatment			
Pyrimidine metabolism	0.151	0.37	0.007
Arginine and proline metabolism	0.151	0.19	0.008
D-glutamine and D-glutamate metabolism	0.151	0.17	0.013
Nitrogen metabolism	0.151	0	0.013
Arginine biosynthesis	0.151	0.51	0.015
Glutathione metabolism	0.173	0.01	0.02
Purine metabolism	0.209	0.09	0.029
Glyoxylate and dicarboxylate metabolism	0.269	0.13	0.045

3. Discussion

The overall reductions in animal performance due to fescue toxicosis are estimated to cost the cattle industry over $2 billion annually [13,14]. Therefore, it is vital to discover management methods to reduce the impact and improve the efficiency of beef production. The objective of the current study was to use untargeted metabolomics to evaluate tall fescue seed and isoflavone consumption effects on metabolic intermediates, outputs, and pathways in the rumen and serum.

The metabolomes of the rumen and circulatory environments were first compared, independent of treatment groups, which observed distinctly unique metabolomes according to principal coordinate and abundance analyses. Highly abundant metabolites in each environment were not shared or only present in low abundances between the two environments. The metabolites identified between these different body systems are likely a result of the specific physiological functions of each system in the ruminant. The microbiome is a major contributor to rumen metabolome, as it supplies over 70% of the ruminant's required nutrients [15]. These microbes are highly metabolically active in order to break down feedstuffs and release metabolites to complement host metabolism of which metabolites originate from the plants and other feedstuffs consumed [16]. Therefore, the majority of metabolites identified in the rumen are of xenobiotic origin. By evaluating the rumen metabolome, the effects of tall fescue seed and isoflavone consumption on rumen microbial metabolic processes can be inferred. The serum metabolites, however, are a result of absorbed metabolic products from the rumen and other organs. Tissues throughout the body produce intermediary metabolites from protein, carbohydrate, and lipid metabolism for energy production to perform physiological functions. These metabolites are then absorbed into the blood and can travel through the circulatory system to other tissues for further catabolic or anabolic processing. Therefore, the metabolome of the circulatory system is typically dominated by endogenous metabolites. Because of this systemic nature, metabolites in blood have been used as potential biomarkers to predict feed utilization [17] and production parameters [18], as well as evaluate responses to disease [19,20] and stress [21]. Evaluating the serum metabolome will determine the systemic metabolic response to tall fescue seed and isoflavone supplementation. Together, the effects on individual metabolites and metabolic pathways in rumen fluid and serum will determine how alterations in microbial and host metabolism contribute to symptoms of fescue toxicosis or the benefits isoflavones may contribute to mitigate these detrimental impacts.

Reductions in average daily gain and delayed development of beef cattle are a major consequence of fescue toxicosis [8,22]. The rumen microbiome is crucial for providing nutrients needed by the host for energy requirements and muscle development. As the microbiome has previously been shown to be affected by consuming endophyte infected tall fescue [12,23], the metabolites and other products produced by the rumen microorganisms may be altered, potentially contributing to reductions in growth and feed efficiency. The metabolites produced by the rumen microorganisms are a result of the richness of the rumen microbiome. Several of these metabolites released may be related to the consumption of ergot alkaloids concentrated on the endophyte infected tall fescue seed. Many of the rumen metabolites have a relationship with purine, carbohydrate, and nucleic acid metabolism, such as

hypoxanthine, xylose, and uracil, respectively [24,25]; these metabolites are related to feed efficiency parameters. Clemmons et al. [26] found that these metabolites are bio-indicators of feed efficiency in cattle showing low residual feed intake. Interestingly, they are negatively correlated to seed type in the rumen fluid of the current study; it is evident that animals are being affected by the detrimental symptoms of tall fescue toxicosis, failing to gain weight, and being less feed-efficient. Additionally, we did not observe a large number of different metabolites because of the reduction of the rumen microbiome. As a normal rumen environment, the significant presence of other metabolites, which are crucial for the ergot alkaloids metabolism and production of volatile fatty acids, was expected and improves feed efficiency and rumen microbial richness.

Vasoconstriction, induced by ergot alkaloids, occurs throughout the body, resulting in multiple observed symptoms of fescue toxicosis [4,6]. Specifically, the contractility of the mesenteric vasculature surrounding the digestive tract is affected by the consumption of ergot alkaloids, potentially affecting nutrient absorption and subsequent host metabolism [5]. However, the consumption of isoflavones promotes vasodilation to increase blood flow and mitigate fescue toxicosis effects [10]. Ideally, oxygen and nutrient delivery to tissues is improved, thus benefiting host metabolism. Evaluating serum metabolites during induced fescue toxicosis and treatment with isoflavones may indicate the changes in metabolism systemically. The serum metabolome in the current study was greatly affected by isoflavone treatments with complete separation of animals' global serum metabolomes between treatment groups; no metabolites differed as a result of seed type. Citrulline was identified as having the greatest influence on serum metabolomes between isoflavone treatment groups. Citrulline is an intermediary metabolite in the urea cycle, a metabolic process crucial for providing non-protein nitrogen to the ruminant [27]. As isoflavones inhibit hyper-ammonia producing bacteria in the rumen, this reduces the amount of protein degradation, leading to decreased ammonia and nitrogen availability [11,28]. Multiple metabolic pathways related to the urea cycle such as arginine biosynthesis and metabolism, pyrimidine metabolism, and nitrogen metabolism were affected in serum metabolites by isoflavone treatments. Therefore, the effect of citrulline on the serum metabolome due to isoflavone treatment may be a result of changes in the urea cycle by improving protein availability to the ruminant for muscle development.

Pantothenate was considered to be a major contributor to differences observed in the global serum metabolome among all treatment combinations, but was significantly higher in abundance in steers receiving isoflavone treatment. Previous studies have indicated different levels of pantothenate in the serum of animals differing in feed efficiency, with more feed efficient animals having greater serum levels of pantothenate [17,26]. Pantothenate is a key intermediary metabolite for the formation of Coenzyme A, which is crucial for amino acid and lipid metabolism for ruminant muscle development [29]. Additionally, the majority of metabolic pathways affected by isoflavone treatment in the current study were related to amino acid metabolism and biosynthesis. As animals experiencing fescue toxicosis often have low average daily gains [8], the use of isoflavone supplementation may mitigate the weight gain and growth consequences of fescue toxicosis. The greater amount of available pantothenate in the serum of animals consuming isoflavones, with changes in the urea cycling of the ruminant, may improve growth and muscle development in steers affected by fescue toxicosis.

A classic symptom of fescue toxicosis is a significant reduction of prolactin secretion; this is due to the similar homology of ergot alkaloids with the neurotransmitter dopamine. Ergot alkaloids will act as an agonist by binding dopamine receptors, preventing the release of prolactin [3,30]. Tyrosine is a precursor for the generation of the neurotransmitter dopamine [31]. The current study found tyrosine metabolism to be affected by seed type in the rumen; tyrosine metabolic pathways are influenced as the signals for dopamine production are reduced during fescue toxicosis. Additionally, the study found tryptophan metabolism was affected by seed type in the serum. Tryptophan is a key amino acid in regulating protein synthesis, specifically in muscle development, of multiple species [32,33]. The effects of tryptophan on muscle development are through the IGF-1 pathway [33]. Tryptophan is a precursor to the neurotransmitter serotonin, which stimulates the production of

IGF-1 [34]. Supplementation of rumen protected tryptophan improved weight gain and feed efficiency of ruminants [35,36]. The observed impact of seed type on tryptophan metabolism in the serum may indicate reduced production of serotonin and subsequent IGF-1 signaling for muscle development. Together, the impacts of fescue toxicosis on tyrosine and tryptophan metabolism were also observed previously in the plasma of steers consuming endophyte-infected or endophyte-free seed [37,38]. Therefore, tall fescue seed consumption alters neurotransmitter development, leading to commonly observed symptoms of fescue toxicosis.

4. Conclusions

In conclusion, the rumen metabolome was largely impacted by seed type, while the serum metabolome was influenced by isoflavone supplementation. In the rumen, the impact of the seed type involved carbohydrate and nucleic acids metabolism products of the fescue seed diet inclusion. In the serum, differences in global metabolomes and individual metabolites involved in urea cycling and amino acid metabolic pathways were identified in animals receiving isoflavones and those that did not. Although the low dose of isoflavones administered to cattle indicated effects on the serum and rumen metabolome, further research is needed to determine the effects at other doses. Future applications may lead to the dietary inclusion of isoflavones to reduce the harmful effects of tall fescue toxicosis.

5. Materials and Methods

All experimental procedures involving animals were approved by the University of Tennessee Institutional Animal Care and Use Committee. The ethic approval code (IACUC) was 2540-0617 and was approved on 20 June 2017.

5.1. Experimental Design and Sample Collection

Experimental design, animal treatments, and sample collection methods have been previously described in Melchior et al. [12]. Briefly, this study used 36 purebred Angus steers of approximately eight months of age weighing 250 ± 20 kg from Ames Plantation in Grand Junction, TN. Steers were transported to the Plateau Research and Education Center (PREC) in Crossville, TN for the trial, as previously described [12]. Steers were allowed a 10 d acclimation period to the diet formulated to provide 11.57% crude protein and 76.93% total digestible nutrients (DM basis). The GrowSafe System© (GrowSafe Systems Ltd., Calgary, AB, Canada) was used to monitor feed intake. Prior to the beginning of the trial, steers were genotyped for the DRD2 receptor gene, which can influence cattle's response to fescue toxicity [12]. Using this information, the study was blocked on DRD2 genotype, implementing a randomized complete block design. A 2 × 2 factorial arrangement of treatments was utilized with two types of tall fescue including endophyte-infected (E+) and endophyte-free fescue (E−), and treatment with Promensil© (P+) or without (P−) to provide red clover isoflavones. This combination of treatments resulted in four treatment groups: (1) endophyte-infected seed without Promensil (E+P−), (2) endophyte-infected with Promensil (E+P+), (3) endophyte-free without Promensil (E−P−), and (4) endophyte-free with Promensil (E−P+). Within each genotype block, steers were randomly assigned to treatments with nine steers per treatment group. The feed trial occurred over 21 days. In order to provide a consistent amount of ergot alkaloids, endophyte-infected tall fescue seed heads were incorporated into feed to provide a minimum of 0.011 mg ergovaline plus ergovalinine × kg of body weight^{-1} (BW) per day [3]. Seed heads were ground through a 5 mm screen using a Wiley Mill (Thomas Scientific, Swedesboro, NJ, USA) and included in feed. A total of 943 mg of isoflavones was provided daily before morning feeding based on previously established dosages [10] using a 28.4 g bolus (Torpac, Inc., Fairfield, NJ, USA) to provide 24.7 g of Promensil. Melchior et al. [12] previously reported the analysis and information of the components present in Promensil, and steers' response to endophyte-infected seed and altered performance parameters. On the final day of the trial (day 21), approximately 9 mL of blood was collected from the coccygeal vein using a serum separator tube (Corvac, Sherwood Medical., St. Louis, MO, USA), and approximately 100 mL of rumen content

was collected via oro-gastric lavage. Blood samples were centrifuged at 2000× *g* and 4 °C for 20 min, and serum was transferred to 2 mL microvials and stored at −80 °C until metabolite extractions. Rumen samples were centrifuged at 6000× *g* at 4 °C for 20 min. The supernatant was aspirated and filtered through a 0.22 µm syringe filter, transferred to 2 mL microvials, and stored at −80 °C until metabolite extraction.

5.2. Metabolite Extraction and Identification

Metabolites were extracted and analyzed as previously described [17] at the UTK Biological and Small Molecule Mass Spectrometry Core (BSMMSC). Briefly, 50 µL of filtered rumen fluid and 50 µL of serum from each steer were extracted using 0.1% formic acid in acetonitrile/water/methanol (2:2:1) using a previously described method [39]. Mobile phases consisted of A: 97:3 water/methanol with 11 mM tributylamine and 15 mM acetic acid and B: methanol, and a gradient consisting of the following: 0.0 min, 0% B; 2.5 min 0% B; 5.0 min, 20% B; 7.5 min, 20% B; 13 min, 55% B; 15.5 min, 95% B; 18.5 min, 95% B; 19 min, 0% B; and 25 min, 0% B; Synergy Hydro-RP column (100 × 2 mm, 2.5 µm particle size) was used to separate metabolites. The flow rate was set to a constant 200 µL/min and the column temperature was kept at 25 °C. A Dionex UltiMate 3000 UPLC system (Thermo Fisher Scientific, Waltham, MA) with an autosampler tray maintained at 4 °C was used to introduce a 10 µL sample to an Exactive Plus Orbitrap MS (Thermo Fisher Scientific, Waltham, MA, USA) using negative electrospray ionization (ESI) with a capillary temperature of 300 °C; spray voltage of 3 kV; and nitrogen sheath and sweep gas at 25 and 3 units, respectively. Data acquisition was done in negative ion mode with a full-scan covering the range of 72–1000 *m/z* at 140,000 resolution with automatic gain control of 3×10^6 ions [40]. Metabolites are annotated using exact mass of the [M−H]− (±5 pmm) ion and known retention times (±0.3 min) generated from an in-house curated database. The database was created from the analysis of authentic standards and consisted of 300 compounds across various metabolic pathways, focusing on water soluble metabolites in pathways conserved among a diverse array of organisms.

5.3. Metabolite Identification

Data were analyzed similarly to those of Clemmons et al. [17]. The Xcalibur MS software (Thermo Electron Corp., Waltham, MA) was used to produce raw files, which were then converted to mzML format using ProteoWizard [41]. The software package Metabolomic Analysis and Visualization Engine for LC–MS Data (MAVEN) [42] was used to identify peaks using converted mzML files. MAVEN identifies metabolites based on non-linear retention time correction and calculates peak areas across samples, using a preliminary mass error of ±20 ppm and a retention time window of 5 min. The UTK BSMMSC used a library of 263 retention time-accurate *m/z* pairs taken from MS1 spectra for final metabolite annotations. These are based on expansions of previous work [40] and have been replicated at the UTK BSMMSC. The eluted peak of the annotated metabolite had to be found within 2 min of the expected retention time, and the metabolite mass had to be within ±5 ppm of the expected value to be identified as a known compound. The compound area of each peak was calculated using the Quan Browser function of the Xcalibur MS Software (Thermo Electron Corp., Waltham, MA, USA).

5.4. Data Analysis

Metabolomic data were analyzed using MetaboAnalyst 4.0 [43] and SAS 9.4 (SAS Institute, Cary, NC, USA). For data analysis in MetaboAnalyst, data were first pre-processed. Metabolite data were filtered using interquartile range, normalized by median, log transformed, and auto scaled prior to analysis in MetaboAnalyst 4.0. First, the rumen and serum metabolomes were collectively compared in order to determine similarity of rumen fluid and serum metabolomes for possible overlap or comparison. The rumen and serum metabolomes were visualized using orthogonal partial least squares discriminant analysis (O-PLS-DA) and partial least squares discriminant analysis (PLS-DA) with 2000 permutations. Model fitting for the O-PLS-DA was assessed using R2Y with prediction

power determined using the Q2 metric. A heatmap was generated with the top 25 metabolites to illustrate differences in serum and rumen fluid metabolomes by steer. Next, rumen fluid and serum metabolomes were analyzed separately by treatment combination (i.e., isoflavone × seed type), isoflavone, and seed type. Within each of these, data were visualized via PCA and O-PLS-DA with 2000 permutations, and metabolomes by individual steers were illustrated using heatmaps. Correlation analyses between the top 25 metabolites and treatment groups or combinations were performed for both rumen fluid and serum metabolomes, as well as variable importance in projections (VIP) of the top 25 metabolites. Finally, pathway analyses were performed to determine metabolic pathways that were significantly impacted in rumen fluid and serum by isoflavone or seed type using a global test with relative-betweenness centrality and a reference pathway of Escherichia coli K-12 MG1655 [44].

Raw data were further analyzed in SAS 9.4 (SAS Institute, Cary, NC, USA), First, data were analyzed for normality using the UNIVARIATE procedure, and were considered normal with a Shapiro–Wilk statistic of ≥0.90 and visual observation of histograms and q-q plots. Data that were normally distributed were analyzed with a mixed model analysis of variance (ANOVA) using the GLIMMIX procedure with fixed effects of seed type, isoflavone treatment, and their interaction with the random effect of genotype × isoflavone × seed type. Metabolites that did not follow a normal distribution were fixed ranked and then analyzed using a mixed model ANOVA using the GLIMMIX procedure with fixed effects of seed type, isoflavone treatment, and their interaction with random effect of genotype × isoflavone × seed type.

Supplementary Materials: The following are available online at http://www.mdpi.com/2072-6651/12/12/744/s1, Supplementary File 1: Means and standard error of the means of all metabolites in the rumen fluid between treatment groups; Supplementary File 2: Means and standard error of the means of all metabolites in the serum between treatment groups.

Author Contributions: Conceptualization, E.A.M.-T. and P.R.M.; Formal analysis, B.A.C.; Funding acquisition, P.R.M.; Investigation, T.B.A.-S. and J.F.C.; Methodology, B.A.C., G.E.B., M.D.F., J.L.K., H.J., J.P.G., K.J.M. and P.R.M.; Project administration, P.R.M.; Resources, E.A.M.-T.; Visualization, T.B.A.-S. and B.A.C.; Writing—original draft, T.B.A.-S., B.A.C., J.F.C., K.J.M. and P.R.M.; Writing—review & editing, T.B.A.-S., E.A.M.-T., B.A.C., J.F.C., J.L.K., K.J.M. and P.R.M. All authors have read and agreed to the published version of the manuscript.

Funding: This research was funded by the University of Tennessee CVM, Center for Excellence in Livestock and Human Diseases.

Acknowledgments: We acknowledge the USDA-NIFA Hatch/Multistate Project W4177-TEN00524-Enhancing the Competitiveness and Value of U.S. Beef. We thank Ames Plantation, UT Plateau Research and Education Center, Rebecca Payton, Lezek Wojakiewicz, and Gloria Gellin (USDA-ARS) for their assistance. We also thank Shawn Campagna and Hector Castro at the UTK Biological and Small Molecule Mass Spectrometry Core (BSMMSC).

Conflicts of Interest: The authors declare no conflict of interest.

References

1. Poole, R.K.; Poole, D.H. Impact of Ergot Alkaloids on Female Reproduction in Domestic Livestock Species. *Toxins* **2019**, *11*, 364. [CrossRef] [PubMed]
2. Moore, J.D.; Carlisle, A.E.; Nelson, J.A.; McCulley, R.L. Fungal endophyte infection increases tall fescue's survival, growth, and flowering in a reconstructed prairie. *Restor. Ecol.* **2019**, *27*, 1000–1007. [CrossRef]
3. Klotz, J.L. Activities and Effects of Ergot Alkaloids on Livestock Physiology and Production. *Toxins* **2015**, *7*, 2801–2821. [CrossRef] [PubMed]
4. Strickland, J.R.; Aiken, G.E.; Klotz, J.L. Ergot Alkaloid Induced Blood Vessel Dysfunction Contributes to Fescue Toxicosis. *Forage Grazinglands* **2009**, *7*, 1–7. [CrossRef]
5. Egert, A.M.; Kim, D.H.; Schrick, F.N.; Harmon, D.L.; Klotz, J.L. Dietary exposure to ergot alkaloids decreases contractility of bovine mesenteric vasculature. *J. Anim. Sci.* **2014**, *92*, 1768–1779. [CrossRef]
6. Poole, D.H.; Lyons, S.E.; Poole, R.K.; Poore, M.H. Ergot alkaloids induce vasoconstriction of bovine uterine and ovarian blood vessels. *J. Anim. Sci.* **2018**, *96*, 4812–4822. [CrossRef]
7. Al-Haidary, A.; Spiers, D.; Rottinghaus, G.E.; Garner, G.B.; Ellersieck, M.R. Thermoregulatory ability of beef heifers following intake of endophyte-infected tall fescue during controlled heat challenge. *J. Anim. Sci.* **2001**, *79*, 1780–1788. [CrossRef]

8. Stuedemann, J.A.; Hoveland, C.S. Fescue Endophyte: History and Impact on Animal Agriculture. *J. Prod. Agric.* **1988**, *1*, 39–44. [CrossRef]
9. Roberts, C.A.; Andrae, J. Tall Fescue Toxicosis and Management. *Crop Manag.* **2004**, *3*, 1–18. [CrossRef]
10. Aiken, G.E.; Flythe, M.D.; Kagan, I.A.; Ji, H.; Bush, L.P. Mitigation of Ergot Vasoconstriction by Clover Isoflavones in Goats (Capra hircus). *Front. Vet. Sci.* **2016**, *3*, 17. [CrossRef]
11. Harlow, B.E.; Flythe, M.D.; Kagan, I.A.; Aiken, G.E. Biochanin A (an Isoflavone Produced by Red Clover) Promotes Weight Gain of Steers Grazed in Mixed Grass Pastures and Fed Dried-Distillers' Grains. *Crop Sci.* **2017**, *57*, 506–514. [CrossRef]
12. Melchior, E.A.; Smith, J.K.; Schneider, L.G.; Mulliniks, J.T.; Bates, G.E.; Flythe, M.D.; Klotz, J.L.; Ji, H.; Goodman, J.P.; Lee, A.R.; et al. Effects of endophyte-infected tall fescue seed and red clover isoflavones on rumen microbial populations and physiological parameters of beef cattle. *Transl. Anim. Sci.* **2018**, *3*, 315–328. [CrossRef] [PubMed]
13. Hoveland, C.S. Importance and economic significance of the Acremonium endophytes to performance of animals and grass plant. *Agric. Ecosyst. Environ.* **1993**, *44*, 3–12. [CrossRef]
14. Kallenbach, R.L. BILL E. KUNKLE INTERDISCIPLINARY BEEF SYMPOSIUM: Coping with tall fescue toxicosis: Solutions and realities. *J. Anim. Sci.* **2015**, *93*, 5487–5495. [CrossRef] [PubMed]
15. Bergman, E.N. Energy contributions of volatile fatty acids from the gastrointestinal tract in various species. *Physiol. Rev.* **1990**, *70*, 567–590. [CrossRef] [PubMed]
16. Fontanesi, L. Metabolomics and livestock genomics: Insights into a phenotyping frontier and its applications in animal breeding. *Anim. Front.* **2016**, *6*, 73–79. [CrossRef]
17. Clemmons, B.A.; Mihelic, R.I.; Beckford, R.C.; Powers, J.B.; Melchior, E.A.; McFarlane, Z.D.; Cope, E.R.; Embree, M.M.; Mulliniks, J.T.; Campagna, S.R.; et al. Serum metabolites associated with feed efficiency in black angus steers. *Metabolomics* **2017**, *13*, 147. [CrossRef]
18. Wu, X.; Sun, H.-Z.; Xue, M.; Wang, D.; Guan, L.L.; Liu, J. Serum metabolome profiling revealed potential biomarkers for milk protein yield in dairy cows. *J. Proteom.* **2018**, *184*, 54–61. [CrossRef]
19. Aich, P.; Jalal, S.; Czuba, C.; Schatte, G.; Herzog, K.; Olson, D.J.; Ross, A.R.; Potter, A.A.; Babiuk, L.A.; Griebel, P.J. Comparative Approaches to the Investigation of Responses to Stress and Viral Infection in Cattle. *OMICS A J. Integr. Biol.* **2007**, *11*, 413–434. [CrossRef]
20. Zandkarimi, F.; Vanegas, J.; Fern, X.; Maier, C.S.; Bobe, G. Metabotypes with elevated protein and lipid catabolism and inflammation precede clinical mastitis in prepartal transition dairy cows. *J. Dairy Sci.* **2018**, *101*, 5531–5548. [CrossRef]
21. Liao, Y.; Hu, R.; Wang, Z.; Peng, Q.; Dong, X.; Zhang, X.; Zou, H.; Pu, Q.; Xue, B.; Wang, L. Metabolomics Profiling of Serum and Urine in Three Beef Cattle Breeds Revealed Different Levels of Tolerance to Heat Stress. *J. Agric. Food Chem.* **2018**, *66*, 6926–6935. [CrossRef] [PubMed]
22. Crawford, R.J.; Forwood, J.R.; Belyea, R.L.; Garner, G.B. Relationship between Level of Endophyte Infection and Cattle Gains on Tall Fescue. *J. Prod. Agric.* **1989**, *2*, 147–151. [CrossRef]
23. Mote, R.S.; Hill, N.S.; Skarlupka, J.H.; Turner, Z.B.; Sanders, Z.P.; Jones, D.P.; Suen, G.; Filipov, N.M. Response of Beef Cattle Fecal Microbiota to Grazing on Toxic Tall Fescue. *Appl. Environ. Microbiol.* **2019**, *85*. [CrossRef] [PubMed]
24. Saleem, F.; Bouatra, S.; Guo, A.C.; Psychogios, N.; Mandal, R.; Dunn, S.M.; Ametaj, B.N.; Wishart, D.S. The Bovine Ruminal Fluid Metabolome. *Metabolomics* **2013**, *9*, 360–378. [CrossRef]
25. Artegoitia, V.M.; Foote, A.P.; Lewis, R.M.; Freetly, H.C. Rumen Fluid Metabolomics Analysis Associated with Feed Efficiency on Crossbred Steers. *Sci. Rep.* **2017**, *7*, 1–14. [CrossRef]
26. Clemmons, B.A.; Martino, C.; Powers, J.B.; Campagna, S.R.; Voy, B.H.; Donohoe, D.R.; Gaffney, J.; Embree, M.M.; Myer, P.R. Rumen Bacteria and Serum Metabolites Predictive of Feed Efficiency Phenotypes in Beef Cattle. *Sci. Rep.* **2019**, *9*, 1–8. [CrossRef]
27. Alemneh, T.; Getahun, D.; Akeberegn, D.; Getabalew, M.; Zewdie, D. Urea Metabolism and Recycling in Ruminants. *Biomed. J. Sci. Tech. Res.* **2019**, *20*, 14790–14796. [CrossRef]
28. Flythe, M.D.; Kagan, I. Antimicrobial Effect of Red Clover (Trifolium pratense) Phenolic Extract on the Ruminal Hyper Ammonia-Producing Bacterium, Clostridium sticklandii. *Curr. Microbiol.* **2010**, *61*, 125–131. [CrossRef]
29. Leonardi, R.; Zhang, Y.-M.; Rock, C.O.; Jackowski, S. Coenzyme A: Back in action. *Prog. Lipid Res.* **2005**, *44*, 125–153. [CrossRef]

30. Sibley, D.R.; Creese, I. Interactions of ergot alkaloids with anterior pituitary D-2 dopamine receptors. *Mol. Pharmacol.* **1983**, *23*, 585–593.
31. Fernstrom, J.D. Dietary Precursors and Brain Neurotransmitter Formation. *Annu. Rev. Med.* **1981**, *32*, 413–425. [CrossRef]
32. Lin, F.D.; Smith, T.K.; Bayley, H.S. A Role for Tryptophan in Regulation of Protein Synthesis in Porcine Muscle. *J. Nutr.* **1988**, *118*, 445–449. [CrossRef] [PubMed]
33. Dukes, A.; Davis, C.; El Refaey, M.; Upadhyay, S.; Mork, S.; Arounleut, P.; Johnson, M.H.; Hill, W.D.; Isales, C.M.; Hamrick, M.W. The aromatic amino acid tryptophan stimulates skeletal muscle IGF1/p70s6k/mTor signaling in vivo and the expression of myogenic genes in vitro. *Nutrition* **2015**, *31*, 1018–1024. [CrossRef] [PubMed]
34. Musumeci, G.; Trovato, F.; Avola, R.; Imbesi, R.; Castrogiovanni, P. Serotonin/growth hormone/insulin-like growth factors axis on pre- and post-natal development: A contemporary review. *OA Anat.* **2013**, *1*, 12. [CrossRef]
35. Ma, H.; Cheng, J.; Zhu, X.; Jia, Z. 2011. Effects of rumen-protected tryptophan on performance, nutrient utilization and plasma tryptophan in cashmere goats. *Afr. J. Biotechnol.* **2011**, *10*, 5806–5811.
36. Lee, J.S.; Priatno, W.; Ghassemi Nejad, J.; Peng, D.Q.; Park, J.S.; Moon, J.O.; Lee, H.G. Effect of dietary rumen-protected L-Tryptophan supplementation on growth performance, blood hematological and biochemical profiles, and gene expression in Korean native steers under cold environment. *Animals* **2019**, *9*, 1036. [CrossRef]
37. Mote, R.S.; Hill, N.S.; Uppal, K.; Tran, V.T.; Jones, D.P.; Filipov, N.M. Metabolomics of fescue toxicosis in grazing beef steers. *Food Chem. Toxicol.* **2017**, *105*, 285–299. [CrossRef]
38. Mote, R.S.; Hill, N.S.; Skarlupka, J.H.; Tran, V.T.; Walker, D.I.; Turner, Z.B.; Sanders, Z.P.; Jones, D.P.; Suen, G.; Filipov, N.M. Toxic tall fescue grazing increases susceptibility of the Angus steer fecal microbiota and plasma/urine metabolome to environmental effects. *Sci. Rep.* **2020**, *10*, 2497. [CrossRef]
39. Kamphorst, J.J.; Fan, J.; Lu, W.; White, E.; Rabinowitz, J.D. Liquid Chromatography–High Resolution Mass Spectrometry Analysis of Fatty Acid Metabolism. *Anal. Chem.* **2011**, *83*, 9114–9122. [CrossRef]
40. Lu, W.; Clasquin, M.F.; Melamud, E.; Amador-Noguez, D.; Caudy, A.A.; Rabinowitz, J.D. Metabolomic Analysis via Reversed-Phase Ion-Pairing Liquid Chromatography Coupled to a Stand Alone Orbitrap Mass Spectrometer. *Anal. Chem.* **2010**, *82*, 3212–3221. [CrossRef]
41. Chambers, M.C.; MacLean, B.; Burke, R.D.; Amodei, D.; Ruderman, D.L.; Neumann, S.; Gatto, L.; Fischer, B.; Pratt, B.; Egertson, J.D.; et al. A cross-platform toolkit for mass spectrometry and proteomics. *Nat. Biotechnol.* **2012**, *30*, 918–920. [CrossRef] [PubMed]
42. Clasquin, M.F.; Melamud, E.; Rabinowitz, J.D. LC-MS Data Processing with MAVEN: A Metabolomic Analysis and Visualization Engine. *Curr. Protoc. Bioinform.* **2012**, *37*. [CrossRef]
43. Chong, J.; Soufan, O.; Li, C.; Caraus, I.; Li, S.; Bourque, G.; Wishart, D.S.; Xia, J. MetaboAnalyst 4.0: Towards more transparent and integrative metabolomics analysis. *Nucleic Acids Res.* **2018**, *46*, W486–W494. [CrossRef] [PubMed]
44. Kanehisa, M.; Goto, S.; Sato, Y.; Kawashima, M.; Furumichi, M.; Tanabe, M. Data, information, knowledge and principle: Back to metabolism in KEGG. *Nucleic Acids Res.* **2013**, *42*, D199–D205. [CrossRef]

FISCAL YEAR 2020 – 2021

FINANCIAL REPORT

April 1, 2021 – June 30, 2021

QUARTERLY REPORT

TOBACCO RESEARCH INCOME
INCOME COMPARISON

Fiscal Years	2014-2015	2015-2016	2016-2017	2017-2018	2018-2019	2019-2020	2020-2021
July	$ 13,386.52	$ 139,619.47	$ 157,187.49	$ 2,459.48	$ 120,890.40	$ 141,864.01	$ 136,565.92
August	$ 301,292.71	$ 177,916.68	$ 137,652.03	$ 292,266.42	$ 126,982.37	$ 145,789.42	$ 11,873.82
September	$ 133,527.76	$ 47,768.58	$ 42,873.59	$ 139,414.92	$ 178,553.92	$ 132,169.60	$ 261,157.23
1st QUARTER	**$ 448,206.99**	**$ 365,304.73**	**$ 337,713.11**	**$ 434,140.82**	**$ 426,426.69**	**$ 419,823.03**	**$ 409,596.97**
October	$ 166,587.97	$ 255,006.22	$ 157,120.53	$ 126,862.91	$ 97,793.84	$ 150,849.00	$ 141,682.93
November	$ 74,462.42	$ 127,495.52	$ 251,055.77	$ 123,267.74	$ 128,963.50	$ 117,280.34	$ 135,157.14
December	$ 190,289.54	$ 26,196.02	$ 113,251.82	$ 135,314.04	$ 175,277.00	$ 151,323.23	$ 159,616.92
2nd QUARTER	**$ 431,339.93**	**$ 408,697.76**	**$ 521,428.12**	**$ 385,444.69**	**$ 402,034.34**	**$ 419,452.57**	**$ 436,456.99**
SIX MONTHS	**$ 879,546.92**	**$ 774,002.49**	**$ 859,141.23**	**$ 819,585.51**	**$ 828,461.03**	**$ 839,275.60**	**$ 846,053.96**
January	$ 44,597.62	$ 264,622.53	$ 109,584.57	$ 127,719.90	$ 564,217.88	$ 120,247.87	$ 93,056.96
February	$ 212,408.73	$ 10,472.72	$ 155,644.33	$ 114,047.53	$ 141,118.46	$ 114,095.14	$ 125,797.09
March	$ 133,593.90	$ 255,769.54	$ 159,012.56	$ 159,645.83	$ 122,472.86	$ 403,962.17	$ 143,903.75
3rd QUARTER	**$ 390,600.25**	**$ 530,864.79**	**$ 424,241.46**	**$ 401,413.26**	**$ 827,809.20**	**$ 638,305.18**	**$ 362,757.80**
NINE MONTHS	**$ 1,270,147.17**	**$ 1,304,867.28**	**$ 1,283,382.69**	**$ 1,220,998.77**	**$ 1,656,270.23**	**$ 1,477,580.78**	**$ 1,208,811.76**
April	$ 165,299.42	$ 20,461.50	$ 43,764.59	$ 65,036.15	$ 146,789.57	$ 117,862.64	$ 144,970.47
May	$ 183,052.97	$ 144,713.80	$ 174,933.87	$ 209,087.27	$ 63,797.02	$ 141,525.18	$ 100,238.76
June	$ 137,563.73	$ 288,160.23	$ 242,003.23	$ 168,621.20	$ 250,352.13	$ 138,849.18	$ 211,130.06
4th QUARTER	**$ 485,916.12**	**$ 453,335.53**	**$ 460,701.69**	**$ 442,744.62**	**$ 460,938.72**	**$ 398,237.00**	**$ 456,339.29**
TOTAL INCOME	**$ 1,756,063.29**	**$ 1,758,202.81**	**$ 1,744,084.38**	**$ 1,663,743.39**	**$ 2,117,208.95**	**$ 1,875,817.78**	**$ 1,665,151.05**

FISCAL YEAR 2020-2021 INCOME AND FINANCIAL REPORT KTRDC 4th QUARTER REPORT

Funds Center		Commitment Item	Annual (Revised) Budget	Prior Balance	Current Month Actual	YTD Actual	Available Budget
1235410080	HOLDING ACCOUNT	All Budget Commitmen	$(2,360,000.00)	$(1,454,020.99)	$(211,130.06)	$(1,665,151.05)	$(694,848.95)
1235410080	HOLDING ACCOUNT	All Revenue Commitme	$(2,360,000.00)	$(1,454,020.99)	$(211,130.06)	$(1,665,151.05)	$(694,848.95)
1235410080	HOLDING ACCOUNT	TTL Revenue Excl Tra	$(2,360,000.00)	$(1,454,020.99)	$(211,130.06)	$(1,665,151.05)	$(694,848.95)
1235410080	HOLDING ACCOUNT	State/Local Grants a	$(1,900,000.00)	$(1,454,020.99)	$(211,130.06)	$(1,665,151.05)	$(234,848.95)
1235410080	HOLDING ACCOUNT	Fund Balance	$(460,000.00)				$(460,000.00)
1235410090	KENTUCKY TOBACCO RES	All Budget Commitmen	$1,000.00				$1,000.00
1235410090	KENTUCKY TOBACCO RES	All Expenses Commitm	$1,000.00				$1,000.00
1235410090	KENTUCKY TOBACCO RES	TTL Expense Excl Tra	$1,000.00				$1,000.00
1235410090	KENTUCKY TOBACCO RES	Operating Expense	$1,000.00				$1,000.00
1235410100	ADMINISTRATION	All Budget Commitmen	$260,000.00	$166,338.57	$15,620.33	$181,958.90	$77,905.32
1235410100	ADMINISTRATION	All Expenses Commitm	$260,000.00	$166,338.57	$15,620.33	$181,958.90	$77,905.32
1235410100	ADMINISTRATION	TTL Expense Excl Tra	$260,000.00	$166,338.57	$15,620.33	$181,958.90	$77,905.32
1235410100	ADMINISTRATION	Faculty		$73,562.88	$6,687.52	$80,250.40	$(80,250.40)
1235410100	ADMINISTRATION	Staff		$40,937.88	$5,128.73	$46,066.61	$(46,066.61)
1235410100	ADMINISTRATION	Other Personnel	$-	$76.49		$76.49	$(76.49)
1235410100	ADMINISTRATION	Fringe Benefits		$28,371.42	$3,134.28	$31,505.70	$(31,505.70)
1235410100	ADMINISTRATION	Operating Expense	$260,000.00	$23,389.90	$669.80	$24,059.70	$235,804.52
1235410110	KTRDC PERSONNEL	All Budget Commitmen	$1,046,700.00	$921,613.92	$92,230.15	$1,013,844.07	$32,855.93
1235410110	KTRDC PERSONNEL	All Expenses Commitm	$1,046,700.00	$921,613.92	$92,230.15	$1,013,844.07	$32,855.93
1235410110	KTRDC PERSONNEL	TTL Expense Excl Tra	$1,046,700.00	$921,613.92	$92,230.15	$1,013,844.07	$32,855.93
1235410110	KTRDC PERSONNEL	Staff		$569,100.71	$59,487.32	$628,588.03	$(628,588.03)
1235410110	KTRDC PERSONNEL	Other Personnel		$141,552.88	$19,307.53	$160,860.41	$(160,860.41)
1235410110	KTRDC PERSONNEL	Fringe Benefits		$183,611.67	$21,300.54	$204,912.21	$(204,912.21)
1235410110	KTRDC PERSONNEL	Operating Expense	$1,046,700.00	$27,348.66	$(7,865.24)	$19,483.42	$1,027,216.58

Funds Center		Commitment Item	Annual (Revised) Budget	Prior Balance	Current Month Actual	YTD Actual	Available Budget
1235410120	PUBLICATIONS & TRAVE	All Budget Commitmen	$35,000.00	$10,508.22	$3,835.33	$14,343.55	$20,656.45
1235410120	PUBLICATIONS & TRAVE	All Expenses Commitm	$35,000.00	$10,508.22	$3,835.33	$14,343.55	$20,656.45
1235410120	PUBLICATIONS & TRAVE	TTL Expense Excl Tra	$35,000.00	$10,508.22	$3,835.33	$14,343.55	$20,656.45
1235410120	PUBLICATIONS & TRAVE	Operating Expense	$35,000.00	$10,508.22	$3,835.33	$14,343.55	$20,656.45
1235410130	BUILDING MAINTENANCE	All Budget Commitmen	$116,000.00	$46,093.82	$23,996.08	$70,089.90	$45,910.10
1235410130	BUILDING MAINTENANCE	All Expenses Commitm	$116,000.00	$46,093.82	$23,996.08	$70,089.90	$45,910.10
1235410130	BUILDING MAINTENANCE	TTL Expense Excl Tra	$116,000.00	$46,093.82	$23,996.08	$70,089.90	$45,910.10
1235410130	BUILDING MAINTENANCE	Operating Expense	$116,000.00	$46,093.82	$23,996.08	$70,089.90	$45,910.10
1235410180	SHOP	All Budget Commitmen	$2,000.00	$1,230.01	$41.66	$1,271.67	$521.99
1235410180	SHOP	All Expenses Commitm	$2,000.00	$1,230.01	$41.66	$1,271.67	$521.99
1235410180	SHOP	TTL Expense Excl Tra	$2,000.00	$1,230.01	$41.66	$1,271.67	$521.99
1235410180	SHOP	Operating Expense	$2,000.00	$1,230.01	$41.66	$1,271.67	$521.99
1235410240	LABORATORY EQUIPMENT	All Budget Commitmen	$270,300.00	$671,595.05	$8,509.40	$680,104.45	$(409,804.45)
1235410240	LABORATORY EQUIPMENT	All Revenue Commitme		$6,300.00		$6,300.00	$(6,300.00)
1235410240	LABORATORY EQUIPMENT	Revenue Transfers		$6,300.00		$6,300.00	$(6,300.00)
1235410240	LABORATORY EQUIPMENT	Trans-ID-Equip sales		$6,300.00		$6,300.00	$(6,300.00)
1235410240	LABORATORY EQUIPMENT	All Expenses Commitm	$270,300.00	$665,295.05	$8,509.40	$673,804.45	$(403,504.45)
1235410240	LABORATORY EQUIPMENT	TTL Expense Excl Tra	$270,300.00	$665,295.05	$8,509.40	$673,804.45	$(403,504.45)
1235410240	LABORATORY EQUIPMENT	Operating Expense	$270,300.00	$184,766.75	$75.90	$184,842.65	$85,457.35
1235410240	LABORATORY EQUIPMENT	Capital Outlay		$480,528.30	$8,433.50	$488,961.80	$(488,961.80)
1235410250	UNALLOCATED RESERVE	All Budget Commitmen	$28.00				$28.00
1235410250	UNALLOCATED RESERVE	All Expenses Commitm	$28.00				$28.00
1235410250	UNALLOCATED RESERVE	TTL Expense Excl Tra	$28.00				$28.00
1235410250	UNALLOCATED RESERVE	Operating Expense	$28.00				$28.00

Funds Center		Commitment Item	Annual (Revised) Budget	Prior Balance	Current Month Actual	YTD Actual	Available Budget
1235410280	GENERAL LABORATORY	All Budget Commitmen	$125,000.00	$50,942.72	$4,235.56	$55,178.28	$69,787.48
1235410280	GENERAL LABORATORY	All Expenses Commitm	$125,000.00	$50,942.72	$4,235.56	$55,178.28	$69,787.48
1235410280	GENERAL LABORATORY	TTL Expense Excl Tra	$125,000.00	$50,942.72	$4,235.56	$55,178.28	$69,787.48
1235410280	GENERAL LABORATORY	Operating Expense	$125,000.00	$50,942.72	$4,235.56	$55,178.28	$69,787.48
1235411040	DISCRETIONARY	All Budget Commitmen	$10,000.00	$1,594.78	$139.69	$1,734.47	$8,265.53
1235411040	DISCRETIONARY	All Expenses Commitm	$10,000.00	$1,594.78	$139.69	$1,734.47	$8,265.53
1235411040	DISCRETIONARY	TTL Expense Excl Tra	$10,000.00	$1,594.78	$139.69	$1,734.47	$8,265.53
1235411040	DISCRETIONARY	Operating Expense	$10,000.00	$1,594.78	$139.69	$1,734.47	$8,265.53
1235411310	OUTREACH & COMMUNICA	All Budget Commitmen	$30,000.00	$40,014.52	$(3,178.61)	$36,835.91	$(7,490.59)
1235411310	OUTREACH & COMMUNICA	All Expenses Commitm	$30,000.00	$40,014.52	$(3,178.61)	$36,835.91	$(7,490.59)
1235411310	OUTREACH & COMMUNICA	TTL Expense Excl Tra	$30,000.00	$40,014.52	$(3,178.61)	$36,835.91	$(7,490.59)
1235411310	OUTREACH & COMMUNICA	Other Personnel		$9,730.60	$530.76	$10,261.36	$(10,261.36)
1235411310	OUTREACH & COMMUNICA	Fringe Benefits		$1,949.04	$46.49	$1,995.53	$(1,995.53)
1235411310	OUTREACH & COMMUNICA	Operating Expense	$30,000.00	$28,334.88	$(3,755.86)	$24,579.02	$4,766.30
1235411320	PLANT GENETIC ENGR	All Budget Commitmen	$30,000.00	$29,982.99		$29,982.99	$17.01
1235411320	PLANT GENETIC ENGR	All Expenses Commitm	$30,000.00	$29,982.99		$29,982.99	$17.01
1235411320	PLANT GENETIC ENGR	TTL Expense Excl Tra	$30,000.00	$29,982.99		$29,982.99	$17.01
1235411320	PLANT GENETIC ENGR	Staff		$15,694.88		$15,694.88	$(15,694.88)
1235411320	PLANT GENETIC ENGR	Other Personnel		$3,421.13		$3,421.13	$(3,421.13)
1235411320	PLANT GENETIC ENGR	Fringe Benefits		$8,362.38		$8,362.38	$(8,362.38)
1235411320	PLANT GENETIC ENGR	Operating Expense	$30,000.00	$2,504.60		$2,504.60	$27,495.40

Funds Center		Commitment Item	Annual (Revised) Budget	Prior Balance	Current Month Actual	YTD Actual	Available Budget
1235411340	GENETIC MANIPULATION	All Budget Commitmen	$30,000.00	$30,003.75		$30,003.75	$(3.75)
1235411340	GENETIC MANIPULATION	All Expenses Commitm	$30,000.00	$30,003.75		$30,003.75	$(3.75)
1235411340	GENETIC MANIPULATION	TTL Expense Excl Tra	$30,000.00	$30,003.75		$30,003.75	$(3.75)
1235411340	GENETIC MANIPULATION	Staff		$22,048.33		$22,048.33	$(22,048.33)
1235411340	GENETIC MANIPULATION	Fringe Benefits		$5,357.53		$5,357.53	$(5,357.53)
1235411340	GENETIC MANIPULATION	Operating Expense	$30,000.00	$2,597.89		$2,597.89	$27,402.11
1235411370	PLANT BIOTECH MOLECU	All Budget Commitmen	$30,000.00	$17,902.59	$2,245.29	$20,147.88	$(2,897.62)
1235411370	PLANT BIOTECH MOLECU	All Expenses Commitm	$30,000.00	$17,902.59	$2,245.29	$20,147.88	$(2,897.62)
1235411370	PLANT BIOTECH MOLECU	TTL Expense Excl Tra	$30,000.00	$17,902.59	$2,245.29	$20,147.88	$(2,897.62)
1235411370	PLANT BIOTECH MOLECU	Operating Expense	$30,000.00	$17,902.59	$2,245.29	$20,147.88	$(2,897.62)
1235411380	MOLECULAR GENETICS	All Budget Commitmen	$30,000.00	$9,421.40	$1,515.60	$10,937.00	$19,063.00
1235411380	MOLECULAR GENETICS	All Expenses Commitm	$30,000.00	$9,421.40	$1,515.60	$10,937.00	$19,063.00
1235411380	MOLECULAR GENETICS	TTL Expense Excl Tra	$30,000.00	$9,421.40	$1,515.60	$10,937.00	$19,063.00
1235411380	MOLECULAR GENETICS	Operating Expense	$30,000.00	$9,421.40	$1,515.60	$10,937.00	$19,063.00
1235411390	METABOLIC ENGR.	All Budget Commitmen	$30,000.00		$315.33	$315.33	$29,463.55
1235411390	METABOLIC ENGR.	All Expenses Commitm	$30,000.00		$315.33	$315.33	$29,463.55
1235411390	METABOLIC ENGR.	TTL Expense Excl Tra	$30,000.00		$315.33	$315.33	$29,463.55
1235411390	METABOLIC ENGR.	Operating Expense	$30,000.00		$315.33	$315.33	$29,463.55
1235411410	GREENHOUSE	All Budget Commitmen	$30,000.00	$15,822.82	$11,952.44	$27,775.26	$2,207.77
1235411410	GREENHOUSE	All Expenses Commitm	$30,000.00	$15,822.82	$11,952.44	$27,775.26	$2,207.77
1235411410	GREENHOUSE	TTL Expense Excl Tra	$30,000.00	$15,822.82	$11,952.44	$27,775.26	$2,207.77
1235411410	GREENHOUSE	Other Personnel		$726.44		$726.44	$(726.44)
1235411410	GREENHOUSE	Fringe Benefits		$51.35		$51.35	$(51.35)
1235411410	GREENHOUSE	Operating Expense	$30,000.00	$15,045.03	$11,952.44	$26,997.47	$2,985.56

Funds Center		Commitment Item	Annual (Revised) Budget	Prior Balance	Current Month Actual	YTD Actual	Available Budget
1235411430	PLANT ANALYTIC	All Budget Commitmen	$30,000.00	$399.52	$22,017.11	$22,416.63	$7,583.37
1235411430	PLANT ANALYTIC	All Expenses Commitm	$30,000.00	$399.52	$22,017.11	$22,416.63	$7,583.37
1235411430	PLANT ANALYTIC	TTL Expense Excl Tra	$30,000.00	$399.52	$22,017.11	$22,416.63	$7,583.37
1235411430	PLANT ANALYTIC	Operating Expense	$30,000.00	$399.52	$22,017.11	$22,416.63	$7,583.37
1235411640	GENE DISCOVERY	All Budget Commitmen	$30,000.00	$27,578.95	$2,032.82	$29,611.77	$388.23
1235411640	GENE DISCOVERY	All Expenses Commitm	$30,000.00	$27,578.95	$2,032.82	$29,611.77	$388.23
1235411640	GENE DISCOVERY	TTL Expense Excl Tra	$30,000.00	$27,578.95	$2,032.82	$29,611.77	$388.23
1235411640	GENE DISCOVERY	Staff		$16,142.94	$1,467.54	$17,610.48	$(17,610.48)
1235411640	GENE DISCOVERY	Fringe Benefits		$5,088.69	$462.61	$5,551.30	$(5,551.30)
1235411640	GENE DISCOVERY	Operating Expense	$30,000.00	$6,347.32	$102.67	$6,449.99	$23,550.01
1235411750	REFERENCE CIGARETTES	All Budget Commitmen		$72,730.00		$72,730.00	$(72,730.00)
1235411750	REFERENCE CIGARETTES	All Expenses Commitm		$72,730.00		$72,730.00	$(72,730.00)
1235411750	REFERENCE CIGARETTES	TTL Expense Excl Tra		$72,730.00		$72,730.00	$(72,730.00)
1235411750	REFERENCE CIGARETTES	Operating Expense		$72,730.00		$72,730.00	$(72,730.00)
1235412240	GREENHOUSE EVALUATIO	All Budget Commitmen	$8,547.00	$8,708.97	$84.12	$8,793.09	$(246.09)
1235412240	GREENHOUSE EVALUATIO	All Expenses Commitm	$8,547.00	$8,708.97	$84.12	$8,793.09	$(246.09)
1235412240	GREENHOUSE EVALUATIO	TTL Expense Excl Tra	$8,547.00	$8,708.97	$84.12	$8,793.09	$(246.09)
1235412240	GREENHOUSE EVALUATIO	Other Personnel		$2,977.80		$2,977.80	$(2,977.80)
1235412240	GREENHOUSE EVALUATIO	Fringe Benefits		$206.82		$206.82	$(206.82)
1235412240	GREENHOUSE EVALUATIO	Operating Expense	$8,547.00	$5,524.35	$84.12	$5,608.47	$2,938.53
1235412360	FLAVONOID - SMALLE	All Budget Commitmen	$30,000.00	$23,424.86	$3,124.17	$26,549.03	$2,265.67
1235412360	FLAVONOID - SMALLE	All Expenses Commitm	$30,000.00	$23,424.86	$3,124.17	$26,549.03	$2,265.67
1235412360	FLAVONOID - SMALLE	TTL Expense Excl Tra	$30,000.00	$23,424.86	$3,124.17	$26,549.03	$2,265.67
1235412360	FLAVONOID - SMALLE	Staff		$9,755.20	$1,219.40	$10,974.60	$(10,974.60)
1235412360	FLAVONOID - SMALLE	Fringe Benefits		$2,527.84	$315.98	$2,843.82	$(2,843.82)
1235412360	FLAVONOID - SMALLE	Operating Expense	$30,000.00	$11,141.82	$1,588.79	$12,730.61	$16,084.09

Funds Center		Commitment Item	Annual (Revised) Budget	Prior Balance	Current Month Actual	YTD Actual	Available Budget
1235412690	SMOKELESS TOBACCO	All Budget Commitmen	$37,069.00	$17,943.18	$2,417.06	$20,360.24	$16,708.76
1235412690	SMOKELESS TOBACCO	All Expenses Commitm	$37,069.00	$17,943.18	$2,417.06	$20,360.24	$16,708.76
1235412690	SMOKELESS TOBACCO	TTL Expense Excl Tra	$37,069.00	$17,943.18	$2,417.06	$20,360.24	$16,708.76
1235412690	SMOKELESS TOBACCO	Operating Expense	$37,069.00	$17,943.18	$2,417.06	$20,360.24	$16,708.76
1235412790	JI: PURIFICATION OF	All Budget Commitmen	$41,672.00	$22,158.54	$2,921.04	$25,079.58	$16,119.85
1235412790	JI: PURIFICATION OF	All Expenses Commitm	$41,672.00	$22,158.54	$2,921.04	$25,079.58	$16,119.85
1235412790	JI: PURIFICATION OF	TTL Expense Excl Tra	$41,672.00	$22,158.54	$2,921.04	$25,079.58	$16,119.85
1235412790	JI: PURIFICATION OF	Operating Expense	$41,672.00	$22,158.54	$2,921.04	$25,079.58	$16,119.85
1235412820	FISHER: FARMER BALES	All Budget Commitmen	$13,500.00	$13,501.08	$0.70	$13,501.78	$(1.78)
1235412820	FISHER: FARMER BALES	All Expenses Commitm	$13,500.00	$13,501.08	$0.70	$13,501.78	$(1.78)
1235412820	FISHER: FARMER BALES	TTL Expense Excl Tra	$13,500.00	$13,501.08	$0.70	$13,501.78	$(1.78)
1235412820	FISHER: FARMER BALES	Staff		$6,241.77		$6,241.77	$(6,241.77)
1235412820	FISHER: FARMER BALES	Other Personnel		$3,355.44		$3,355.44	$(3,355.44)
1235412820	FISHER: FARMER BALES	Fringe Benefits		$3,298.68		$3,298.68	$(3,298.68)
1235412820	FISHER: FARMER BALES	Operating Expense	$13,500.00	$605.19	$0.70	$605.89	$12,894.11
1235412840	MARTINEZ: GREENHOUSE	All Budget Commitmen	$5,000.00	$4,347.10	$308.18	$4,655.28	$344.72
1235412840	MARTINEZ: GREENHOUSE	All Expenses Commitm	$5,000.00	$4,347.10	$308.18	$4,655.28	$344.72
1235412840	MARTINEZ: GREENHOUSE	TTL Expense Excl Tra	$5,000.00	$4,347.10	$308.18	$4,655.28	$344.72
1235412840	MARTINEZ: GREENHOUSE	Operating Expense	$5,000.00	$4,347.10	$308.18	$4,655.28	$344.72
1235412940	ZAITLIN: INDUCE EARL	All Budget Commitmen	$20,502.00	$18,117.96	$1,858.52	$19,976.48	$525.52
1235412940	ZAITLIN: INDUCE EARL	All Expenses Commitm	$20,502.00	$18,117.96	$1,858.52	$19,976.48	$525.52
1235412940	ZAITLIN: INDUCE EARL	TTL Expense Excl Tra	$20,502.00	$18,117.96	$1,858.52	$19,976.48	$525.52
1235412940	ZAITLIN: INDUCE EARL	Staff		$3,841.92	$213.43	$4,055.35	$(4,055.35)
1235412940	ZAITLIN: INDUCE EARL	Fringe Benefits		$1,202.38	$66.80	$1,269.18	$(1,269.18)
1235412940	ZAITLIN: INDUCE EARL	Operating Expense	$20,502.00	$13,073.66	$1,578.29	$14,651.95	$5,850.05

Funds Center		Commitment Item	Annual (Revised) Budget	Prior Balance	Current Month Actual	YTD Actual	Available Budget
1235412950	BAILEY: BURNDOWN	All Budget Commitmen	$6,000.00	$5,376.81	$617.59	$5,994.40	$5.60
1235412950	BAILEY: BURNDOWN	All Expenses Commitm	$6,000.00	$5,376.81	$617.59	$5,994.40	$5.60
1235412950	BAILEY: BURNDOWN	TTL Expense Excl Tra	$6,000.00	$5,376.81	$617.59	$5,994.40	$5.60
1235412950	BAILEY: BURNDOWN	Operating Expense	$6,000.00	$5,376.81	$(379.36)	$4,997.45	$1,002.55
1235412950	BAILEY: BURNDOWN	Capital Outlay			$996.95	$996.95	$(996.95)
1235413180	KROU: ABS CEMB	All Budget Commitmen	$20,000.00	$16,035.75	$4,385.57	$20,421.32	$(421.32)
1235413180	KROU: ABS CEMB	All Expenses Commitm	$20,000.00	$16,035.75	$4,385.57	$20,421.32	$(421.32)
1235413180	KROU: ABS CEMB	TTL Expense Excl Tra	$20,000.00	$16,035.75	$4,385.57	$20,421.32	$(421.32)
1235413180	KROU: ABS CEMB	Other Personnel		$10,504.20	$4,201.68	$14,705.88	$(14,705.88)
1235413180	KROU: ABS CEMB	Operating Expense	$20,000.00	$5,531.55	$183.89	$5,715.44	$14,284.56
1235413200	PERRY: PROD MAL	All Budget Commitmen	$22,173.00	$24,173.32	$1,958.55	$26,131.87	$(3,958.87)
1235413200	PERRY: PROD MAL	All Expenses Commitm	$22,173.00	$24,173.32	$1,958.55	$26,131.87	$(3,958.87)
1235413200	PERRY: PROD MAL	TTL Expense Excl Tra	$22,173.00	$24,173.32	$1,958.55	$26,131.87	$(3,958.87)
1235413200	PERRY: PROD MAL	Other Personnel		$14,624.23	$1,698.96	$16,323.19	$(16,323.19)
1235413200	PERRY: PROD MAL	Fringe Benefits		$438.37	$148.83	$587.20	$(587.20)
1235413200	PERRY: PROD MAL	Operating Expense	$22,173.00	$9,110.72	$110.76	$9,221.48	$12,951.52
1235413210	PATRA: ROOT TO LEAF	All Budget Commitmen	$19,509.00	$15,477.92	$4,436.46	$19,914.38	$(405.38)
1235413210	PATRA: ROOT TO LEAF	All Expenses Commitm	$19,509.00	$15,477.92	$4,436.46	$19,914.38	$(405.38)
1235413210	PATRA: ROOT TO LEAF	TTL Expense Excl Tra	$19,509.00	$15,477.92	$4,436.46	$19,914.38	$(405.38)
1235413210	PATRA: ROOT TO LEAF	Staff		$3,878.96		$3,878.96	$(3,878.96)
1235413210	PATRA: ROOT TO LEAF	Fringe Benefits		$1,227.90		$1,227.90	$(1,227.90)
1235413210	PATRA: ROOT TO LEAF	Operating Expense	$19,509.00	$10,371.06	$4,436.46	$14,807.52	$4,701.48

Kentucky Tobacco
Research & Development Center